

Supporting Information

Increasing the triplet lifetime and extending the ground-state absorption of biscyclometalated Ir(III) complexes for reverse saturable absorption and photodynamic therapy applications

Chengzhe Wang,^a Levi Lystrom,^a Huimin Yin,^b Marc Hetu,^b Svetlana Kilina,^a Sherri A. McFarland,^{*b,c} Wenfang Sun^{*a}

^a Department of Chemistry and Biochemistry, North Dakota State University, Fargo, ND 58108-6050, USA. E-mail: Wenfang.Sun@ndsu.edu

^b Department of Chemistry, Acadia University, 6 University Avenue, Wolfville, NS B4P 2R6, Canada. E-mail: sherri.mcfarland@acadiau.ca

^c Department of Chemistry and Biochemistry, University of North Carolina at Greensboro, Greensboro, NC 27402-6170, USA. E-mail: samcfarl@uncg.edu

Experimental Details

Materials and characterizations

All of the reagents and solvents for synthesis were purchased from Alfa Aesar and used as is unless otherwise stated. Spectrophotometric grade solvents purchased from VWR International were used for spectroscopic studies. Silica gels (230-400 mesh) used for chromatography were purchased from Sorbent Technology. Synthesis of the ligands and complexes followed the published procedures for the same or similar compounds,^{1,2} and the synthetic route was shown in Scheme 1 in the main text. The intermediate compounds were characterized by ¹H NMR spectroscopy, while the ligands were characterized by ¹H NMR, and elemental analyses and the Ir(III) complexes were characterized by ¹H NMR, HRMS, and elemental analyses.

¹H NMR spectra were obtained on a Varian Oxford-500 VNMR spectrometer using CDCl₃ as the solvent, with tetramethylsilane as internal standard. ESI-HRMS analyses were performed on a Bruker BioTOF III mass spectrometer or a Waters Synapt G2-Si high resolution mass spectrometer. Elemental analyses were carried out by NuMega Resonance Laboratories, Inc. in San Diego, California.

1,10-phenanthroline-5,6-dione (pdo). Sulfuric acid (20 mL) was stirred in a flask then cooled with ice-water bath. A mixture of 1,10-phenanthroline (1.0 g, 5.5 mmol) and NaBr (5.7 g, 55 mmol) was slowly added in several small portions. HNO₃ (10 mL) was then introduced into the solution. The mixture was kept in ice-water bath for 10 min and an oil-water separator was connected to the flask. The mixture was heated to 90 °C for 2 h. After cooling, the crude product was poured onto ice, then neutralized with NaHCO₃ to pH = 6-7. The suspension was extracted using CH₂Cl₂. The organic layer was concentrated and then recrystallized with 95% ethanol. Yellow needles were obtained as the product (1.17 g, 100%). ¹H NMR (CDCl₃, 400 MHz) δ 9.13 (dd, *J* = 4.7, 1.9 Hz, 2H), 8.51 (dd, *J* = 7.9, 1.9 Hz, 2H), 7.59 (dd, *J* = 7.9, 4.7 Hz, 2H).

General synthetic procedure for pyrazine derivatives. Diketone (dpo, or benzyl, 1 eq) and diimine (ethane-1,2-diamine, benzene-1,2-diamine, or naphthalene-2,3-diamine, 1 eq) were added to absolute ethanol (30 mL). The mixture was refluxed under nitrogen for 12 h. After concentrating, the mixture was directly recrystallized with ethanol to get the product.

dpq. Dpq (150 mg, 0.71 mmol) and 1,2-diaminoethane (47 mg, 0.78 mmol) in absolute ethanol (20 mL) gave product as yellow crystals (77 mg, 46%). ¹H NMR (CDCl₃, 500 MHz) δ 9.52 (dd, *J* = 8.1, 1.9 Hz, 2H), 9.31 (dd, *J* = 4.4, 1.8 Hz, 2H), 9.00 (s, 2H), 7.81 (dd, *J* = 8.2, 4.4 Hz, 2H); elemental analysis calcd (%) for C₁₄H₈N₄ · 0.15H₂O: C, 71.57; H, 3.56; N, 23.85; found: C, 71.94; H, 3.95; N, 23.66.

dppz. dpq (105 mg, 0.5 mmol) and 1,2-diaminobenzene (59 mg, 0.55 mmol) in absolute ethanol (20 mL) gave product as yellow solid (130 mg, 92%). ¹H NMR (CDCl₃, 500 MHz) δ 9.68 (dd, *J* = 8.1, 1.8 Hz, 2H), 9.29 (dd, *J* = 4.4, 1.8 Hz, 2H), 8.39 (dd, *J* = 6.5, 3.4 Hz, 2H), 7.94 (dd, *J* = 6.5, 3.4 Hz, 2H), 7.81 (dd, *J* = 8.1, 4.5 Hz, 2H); elemental analysis calcd (%) for C₁₈H₁₀N₄ · 0.5H₂O: C, 74.21; H, 3.81; N, 19.23; found: C, 74.55; H, 4.20; N, 19.43.

dppn. dpq (200 mg, 0.95 mmol) and 2,3-diaminonaphthalene (166.1 mg, 1.05 mmol) in absolute ethanol gave product as orange solid (222 mg, 71%). ¹H NMR (CDCl₃, 500 MHz) δ 9.68 (dd, *J* = 8.0, 1.8 Hz, 2H), 9.27 (dd, *J* = 4.6, 1.8 Hz, 2H), 8.99 (s, 2H), 8.23 (dd, *J* = 6.5, 3.3 Hz, 2H), 7.81 (dd, *J* = 8.1, 4.4 Hz, 2H), 7.64 (dd, *J* = 6.6, 3.2 Hz, 2H); elemental analysis calcd (%) for C₂₂H₁₂N₄ · 0.1 · C₇H₁₆ · 1.3 H₂O: C, 74.53; H, 4.46; N, 15.32; found: C, 74.26; H, 4.33; N, 15.26.

dpqx. Benzil (580 mg, 2.77 mmol) and benzene-1,2-diamine (300 mg, 2.77 mmol) gave product as white solid (740 mg, 95%). ¹H NMR (CDCl₃, 500 MHz) δ 8.19 (dd, *J* = 6.4, 3.3 Hz, 2H), 7.78 (dd, *J* = 6.4, 3.3 Hz, 2H), 7.55-7.49 (m, 3H), 7.40-7.31 (m, 6H); elemental analysis calcd (%) for C₂₀H₁₄N₂: C, 85.08; H, 5.00; N, 9.92; found: C, 84.71; H, 5.39; N, 10.32.

dpbq. Benzil (0.5 g, 2.38 mmol) and naphthalene-2,3-diamine (377 mg, 2.38 mmol) gave product as white solid (637 mg, 81%). ¹H NMR (CDCl₃, 500 MHz) δ 8.75 (s, 2H), 8.16-8.10 (m, 2H), 7.61-7.54 (m, 6H), 7.43-7.32 (m, 6H); elemental analysis calcd (%) for C₂₄H₁₆N₂: C, 86.72; H, 4.85; N, 8.43; found: C, 86.35; H, 5.21; N, 8.64.

dpp. Instead of getting the desired ligand dpp, the reaction of benzil (0.8 g, 3.8 mmol) and ethane-1,2-diamine (228 mg, 3.8 mmol) gave an intermediate product, 5,6-diphenyl-2,3-dihydropyrazine as a yellow solid (815 mg, 92%) via column purification (silica gel, hexanes/CH₂Cl₂ = 5/1, v/v). ¹H NMR (CDCl₃, 500 MHz) δ 7.40 (d, *J* = 8.3 Hz, 4H), 7.33-7.29 (m, 2H), 7.24 (d, *J* = 8.0 Hz, 4H), 3.70 (s, 4H).

This intermediate was dissolved in PEG-600 with catalytic amount of *t*-BuOK. Then the mixture was bubbled with air and heated to 120 °C for 3 d. After cooling to r.t, water was added to the reaction mixture to precipitate out the crude product. Pure dpp was obtained after recrystallization in 95% ethanol as yellow powder (720 mg, 89%). ¹H NMR (CDCl₃, 500 MHz) δ 8.61 (s, 2H), 7.48-7.43 (m, 4H), 7.36-7.28 (m, 6H).

General synthetic procedure for Ir(III) dimers. The cyclometalating ligands (piq, dpp, dpq, or dpbq; 2 eq) and IrCl₃·xH₂O (1 eq) were added to a mixture of 2-ethoxyethanol and water (3:1, v/v). The mixture was purged with nitrogen and heated to reflux for 24 h. The mixture was cooled to r.t. and poured into water (100 mL). The precipitate was filtered then washed with hexanes to obtain red to dark red solid.

[Ir(piq)₂]₂Cl₂. Reaction of piq (200 mg, 0.971 mmol) and IrCl₃·xH₂O (190 mg, 0.485 mmol) in a mixture of 2-ethoxyethanol (15 mL) and water (4 mL) gave red powders as the product (209 mg, 29%). ¹H NMR (CDCl₃, 500 MHz) δ 9.04 (d, *J* = 6.4 Hz, 4H), 8.97 (d, *J* = 8.5 Hz, 2H), 8.12 (d, *J* = 8.0 Hz, 4H), 7.89-7.79 (m, 10H), 7.76 (ddd, *J* = 8.4, 6.4, 2.0 Hz, 4H), 6.81 (ddd, *J* = 8.1, 7.1, 1.3 Hz, 4H), 6.55 (d, *J* = 6.4 Hz, 4H), 6.50 (t, *J* = 7.4 Hz, 2H), 6.03 (dd, *J* = 7.9, 1.0 Hz, 6H).

[Ir(dpp)₂]₂Cl₂. Reaction of dpp (105 mg, 454 μmol) and IrCl₃·xH₂O (80 mg, 227 μmol) in a mixture of 2-ethoxyethanol (18 mL) and water (6 mL) gave yellow powders as the crude product (126 mg, 80%). This dimer could not be purified due to poor solubility. It was used directly for the next step reaction.

[Ir(dpqx)₂]₂Cl₂. Reaction of dpq (100 mg, 0.354 mmol) and IrCl₃·xH₂O (62.4 mg, 0.177 mmol) in a mixture of 2-ethoxyethanol (15 mL) and water (5 mL) gave dark red solid as the product (120 mg, 86%). ¹H NMR (CDCl₃, 500 MHz) δ 8.42 (d, *J* = 8.7 Hz, 4H), 8.07 (d, *J* = 53.1 Hz, 8H), 7.81-7.56 (m, 16H), 7.28 (t, *J* = 7.5 Hz, 4H), 6.87 (d, *J* = 8.1 Hz, 4H), 6.70 (t, *J* = 7.8 Hz, 4H), 6.44 (t, *J* = 7.5 Hz, 4H), 6.17 (t, *J* = 7.4 Hz, 4H), 5.66 (d, *J* = 7.7 Hz, 4H).

[Ir(dpbq)₂]₂Cl₂. Reaction of dpbq (180 mg, 0.54 mmol) and IrCl₃·xH₂O (95 mg, 0.27 mmol) in a mixture of 2-ethoxyethanol (15 mL) and water (5 mL) gave dark red solid as the product (130 mg, 54%). ¹H NMR (CDCl₃, 500 MHz) δ 8.92 (s, 4H), 8.26 (d, *J* = 7.5 Hz, 4H), 7.98 (d, *J* = 8.3 Hz, 4H), 7.94 (d, *J* = 6.4 Hz, 4H), 7.86 (s, 4H), 7.78-7.62 (m, 12H), 7.35 (d, *J* = 7.4 Hz, 4H), 7.31 (d, *J* = 8.9 Hz, 4H), 7.06 (d, *J* = 8.3 Hz, 4H), 6.37 (q, *J* = 8.1 Hz, 8H), 5.98 (t, *J* = 7.5 Hz, 4H), 5.57 (d, *J* = 7.9 Hz, 4H).

General synthetic procedure for Ir(III) complexes 1-6. The Ir(III) dimer (1 eq), diimine ligand (2 eq), and AgSO₃CF₃ (2.5 eq) were added to 2-ethoxyethanol or a mixture of dichloromethane and methanol (v/v = 2/1). It was purged with nitrogen and heated to reflux for 16 h. The mixture was cooled to r.t. and NH₄PF₆ (20 eq) was added. After stirring for 1 h at r.t., solvent was removed and the crude product was purified via column chromatography (silica gel, CH₂Cl₂/ethyl acetate = 50-100/1, v/v). The product was further purified by recrystallization in CH₂Cl₂ and hexanes.

Complex 1. Reaction of [Ir(piq)₂]₂Cl₂ (100 mg, 0.079 mmol), dpq (36.7 mg, 0.158 mmol), and AgSO₃CF₃ (40.6 mg, 0.158 mmol) in 20 mL 2-ethoxyethanol gave orange powders as the product (83.0 mg, 76%). ¹H NMR (CDCl₃, 500 MHz) δ 9.71 (d, *J* = 8.3 Hz, 2H), 9.14 (s, 2H), 8.95 (d, *J* = 8.3 Hz, 2H), 8.31 (d, *J* = 8.1 Hz, 2H), 8.17 (d, *J* = 5.1 Hz, 2H), 7.90 (dd, *J* = 8.3, 5.3 Hz, 2H), 7.85 (d, *J* = 7.5 Hz, 2H), 7.75 (quintet, *J* = 7.8 Hz, 4H), 7.35 (d, *J* = 6.5 Hz, 2H), 7.29 (d, *J* = 6.5 Hz, 2H), 7.17 (t, *J* = 7.7 Hz, 2H), 6.97 (t, *J* = 7.4 Hz, 2H), 6.40 (d, *J* = 7.6 Hz, 2H). HRMS (ESI): *m/z* calc for [C₄₄H₂₈IrN₆]⁺: 833.2007; found: 833.1991. Elemental analysis calcd (%) for C₄₄H₂₈F₆IrN₆P: C, 54.38; H, 2.89; N, 8.59; found: C, 54.46; H, 3.26; N, 8.44.

Complex 2. Reaction of [Ir(piq)₂]₂Cl₂ (100 mg, 0.079 mmol), dppz (44.6 mg, 0.158 mmol), and AgSO₃CF₃ (40.6 mg, 0.158 mmol) in 20 mL 2-ethoxyethanol gave red solids as product (97.0 mg, 60%). ¹H NMR (CDCl₃, 500 MHz) δ 9.74 (d, *J* = 8.2 Hz, 2H), 8.93 (d, *J* = 8.5 Hz, 2H), 8.34-8.25 (m, 4H), 8.17 (d, *J* = 5.1 Hz, 2H), 7.92-7.85 (m, 4H), 7.83 (d, *J* = 7.9 Hz, 2H), 7.74-7.67 (m, 4H), 7.42 (d, *J* = 6.4 Hz, 2H), 7.33 (d, *J* = 6.6 Hz, 2H), 7.13 (t, *J* = 7.7 Hz, 2H), 6.94 (t, *J* = 7.5 Hz, 2H), 6.44 (d, *J* = 7.6 Hz, 2H). HRMS (ESI): *m/z* calc for [C₄₈H₃₀IrN₆]⁺: 883.2164; found: 883.2167. Elemental analysis calcd (%) for C₄₈H₃₀F₆IrN₆P · 0.8CH₃CN: C, 56.16; H, 3.08; N, 8.98; found: C, 56.55; H, 3.40; N, 8.63.

Complex 3. Reaction of [Ir(piq)₂]₂Cl₂ (100 mg, 0.079 mmol), dppn (52.5 mg, 0.158 mmol), and AgSO₃CF₃ (40.6 mg, 0.158 mmol) in 20 mL 2-ethoxyethanol gave orange powders as product (60.0 mg, 35%). ¹H NMR (CDCl₃, 500 MHz) δ 9.78 (d, *J* = 8.0 Hz, 2H), 8.97 (d, *J* = 10.7 Hz, 3H), 8.33 (d, *J* = 8.2 Hz, 3H), 8.13 (d, *J* = 4.7 Hz, 3H), 7.91-7.84 (m, 4H), 7.80-7.70 (m, 5H),

7.60 (d, $J = 7.0$ Hz, 1H), 7.48 (d, $J = 6.6$ Hz, 1H), 7.35 (d, $J = 6.5$ Hz, 2H), 7.18 (t, $J = 7.8$ Hz, 3H), 6.98 (t, $J = 7.5$ Hz, 3H), 6.42 (d, $J = 7.6$ Hz, 2H). HRMS (ESI): m/z calc for $[\text{C}_{52}\text{H}_{32}\text{IrN}_6]^+$: 933.2321; found: 933.2314. Elemental analysis calcd (%) for $\text{C}_{52}\text{H}_{32}\text{F}_6\text{IrN}_6\text{P} \cdot 0.3\text{H}_2\text{O}$: C, 57.94; H, 2.99; N, 7.80; found: C, 57.65; H, 3.38; N, 7.60.

Complex 4. Reaction of dppn (52 mg, 0.156 mmol), $[\text{Ir}(\text{dpp})_2]_2\text{Cl}_2$ (120 mg, 0.086 mmol) and AgSO_3CF_3 (55.8 mg, 0.217 mmol) in a mixture of CH_2Cl_2 (30 mL) and CH_3OH (15 mL) gave yellow powders as product (26.0 mg, 13%). ^1H NMR ($\text{DMSO}-d_6$, 400 MHz) δ 9.87-9.79 (m, 2H), 9.28 (s, 2H), 8.46 (dd, $J = 6.6, 3.3$ Hz, 2H), 8.31-8.25 (m, 4H), 8.24 (d, $J = 3.3$ Hz, 2H), 7.86 (d, $J = 3.3$ Hz, 2H), 7.80 (dd, $J = 6.6, 3.2$ Hz, 2H), 7.61 (s, 10H), 7.02 (td, $J = 7.4, 1.4$ Hz, 2H), 6.88 (dd, $J = 8.2, 1.4$ Hz, 2H), 6.77 (ddd, $J = 8.3, 7.2, 1.3$ Hz, 2H), 6.53 (d, $J = 7.2$ Hz, 2H). HRMS (ESI): m/z calc for $[\text{C}_{54}\text{H}_{34}\text{IrN}_8]^+$: 987.2540; found: 987.2515. Elemental analysis calcd (%) for $\text{C}_{54}\text{H}_{34}\text{F}_6\text{IrN}_8\text{P}$: C, 57.29; H, 3.03; N, 9.90; found: C, 57.13; H, 3.40; N, 9.58.

Complex 5. Reaction of $[\text{Ir}(\text{dpqx})_2]_2\text{Cl}_2$ (120 mg, 0.076 mmol), dppn (50.6 mg, 0.152 mmol) and AgSO_3CF_3 (39.1 mg, 0.152 mmol) in a mixture of CH_2Cl_2 (40 mL) and CH_3OH (20 mL) gave orange solids as product (127 mg, 68%). ^1H NMR (CDCl_3 , 500 MHz) δ 9.26 (d, $J = 5.2$ Hz, 2H), 9.19 (d, $J = 8.1$ Hz, 2H), 8.36 (dd, $J = 8.1, 5.2$ Hz, 2H), 7.98 (d, $J = 8.5$ Hz, 6H), 7.91 (d, $J = 8.2$ Hz, 2H), 7.80 (t, $J = 7.5$ Hz, 4H), 7.74 (t, $J = 7.5$ Hz, 2H), 7.51 (t, $J = 9.7$ Hz, 4H), 7.42 (t, $J = 7.6$ Hz, 2H), 7.32 (d, $J = 8.3$ Hz, 2H), 7.29-7.22 (m, 4H), 6.90 (t, $J = 7.8$ Hz, 2H), 6.81 (t, $J = 7.4$ Hz, 2H), 6.62 (d, $J = 7.7$ Hz, 2H). HRMS (ESI): m/z calc for $[\text{C}_{62}\text{H}_{38}\text{IrN}_8]^+$: 1087.2854; found: 1087.2802. Elemental analysis calcd (%) for $\text{C}_{62}\text{H}_{38}\text{F}_6\text{IrN}_8\text{P} \cdot 2.5\text{CH}_3\text{OH}$: C, 59.03; H, 3.69; N, 8.54; found: C, 58.90; H, 3.70; N, 8.91.

Complex 6. Reaction of $[\text{Ir}(\text{dpbq})_2]_2\text{Cl}_2$ (100 mg, 0.056 mmol), dppn (37.3 mg, 0.112 mmol) and AgSO_3CF_3 (28.8 mg, 0.112 mmol) in a mixture of CH_2Cl_2 (40 mL) and CH_3OH (20 mL) gave dark red solids as product (64.7 mg, 43%). ^1H NMR (CDCl_3 , 500 MHz) δ 9.36 (d, $J = 4.6$ Hz, 2H), 9.19 (d, $J = 8.1$ Hz, 2H), 8.55 (t, $J = 7.0$ Hz, 2H), 8.51 (s, 2H), 8.05 (d, $J = 6.8$ Hz, 6H), 7.90 (s, 2H), 7.85 (t, $J = 7.7$ Hz, 4H), 7.78 (d, $J = 7.4$ Hz, 2H), 7.74 (d, $J = 9.1$ Hz, 4H), 7.50-7.31 (m, 10H), 6.90 (t, $J = 7.5$ Hz, 2H), 6.77 (t, $J = 7.4$ Hz, 2H), 6.69 (d, $J = 7.6$ Hz, 2H). HRMS (ESI): m/z calc for $[\text{C}_{70}\text{H}_{42}\text{IrN}_8]^+$: 1187.3168; found: 1187.3187. Elemental analysis calcd (%) for $\text{C}_{70}\text{H}_{42}\text{F}_6\text{IrN}_8\text{P} \cdot 1.4\text{CH}_2\text{Cl}_2$: C, 59.09; H, 3.11; N, 7.72; found: C, 58.78; H, 3.16; N, 8.11.

Photophysical studies

UV-vis absorption was measured on a Shimadzu UV-2501 spectrophotometer. The steady-state emission spectra were obtained on a Horiba Jobin Yvon FluoroMax-4 spectrofluorometer. The emission quantum yields of complexes were measured in degassed solutions by relative actinometry method,³ with a degassed $[\text{Ru}(\text{bpy})_3]\text{Cl}_2$ acetonitrile solution ($\Phi_{\text{em}} = 0.097$, $\lambda_{\text{ex}} = 436$ nm) being used as the reference.⁴ An Edinburgh LP920 laser flash photolysis spectrometer was used to measure the nanosecond transient difference absorption spectra (TA), the triplet excited-state lifetimes, and the triplet excited-state quantum yields. It was pumped with the third harmonic output (355 nm) of a Nd:YAG laser (Quantel Brilliant, pulsewidth: 4.1 ns, repetition

rate was set to 1 Hz). The solutions were purged with nitrogen for 40 min to eliminate oxygen prior to each measurement of emission and TA. The triplet excited-state molar extinction coefficients (ϵ_T) at the TA band maximum was estimated according to the singlet depletion method;⁵ and the triplet excited-state quantum yield Φ_T was deduced by the relative actinometry,⁶ using silicon naphthalocyanine (SiNc) in benzene as the reference ($\epsilon_{590} = 70\,000\text{ M}^{-1}\text{ cm}^{-1}$, $\Phi_T = 0.20$).⁷

Nonlinear transmission measurement

Samples were prepared in a 2-mm cuvette with acetonitrile as the solvent. Their linear transmission was adjusted to 80% at 532 nm. The nonlinear transmission experiments were performed on a Quantel Brilliant 4.1 ns laser at its 532 nm mode with a repetition rate of 10 Hz. The experimental details were reported earlier.⁸

Computational methods

Gaussian09 quantum chemistry software⁹ was used for all calculations. Optimization of the singlet ground state of all considered complexes was done using density functional theory (DFT) employing hybrid functional PBE1PBE,¹⁰ and combined basis set LANL2DZ/6-31g*, where LANL2DZ was used for Ir(III) and 6-31g* was used for C, N and H atoms. This methodology had shown reasonable accuracy in descriptions of photophysical properties of similar complexes.¹¹ Conductor Polarized Continuum Model (CPCM)¹² with acetonitrile solvent was implemented for all calculations to describe the effect of solvent on the geometry, electronic levels and optical transitions. To compute linear absorption, linear response time-dependent DFT (TDDFT) was used with the same functional and basis sets used at the ground state calculations.¹³ To reach the energy window needed to computational describe the experimental absorption, the lowest 100 excited states were calculated. Each transition was dressed by a Gaussian Bell curve with the line width of $\sigma = 0.1\text{ eV}$. The obtained profile agrees both quantitatively and qualitatively with the experimental spectra. To better understand the type of optical transitions from the ground state (S_0) to the excited state (S_n), natural transition orbitals (NTOs)¹⁴ were computed using Gaussian09⁹ and visualized using the GaussView software.¹⁵ Excited state orbitals, NTOs, were also compared with the ground state molecular orbitals (MOs).

Cell culture

HL-60. HL-60 human promyelocytic leukemia cells (ATCC CCL-240) were cultured at 37 °C under 5% CO₂ in RPMI 1640 (Mediatech Media MT-10-040-CV) supplemented with 20% FBS (PAA Laboratories, A15-701) and were passaged 3–4 times per week according to standard aseptic procedures. Cultures were started at 200,000 cells/mL in 25 cm² tissue culture flasks and were subcultured when growth reached 800,000 cells/mL to avoid senescence associated with prolonged high cell density. Complete media was prepared in 200-mL portions as needed by combining RPMI 1640 (160 mL) and FBS (40 mL, prealiquoted and heat inactivated), in a 250-mL Millipore vacuum stericup (0.22 μm) and filtering.

SK-MEL-28. Adherent SK-MEL-28 malignant melanoma cells (ATCC HTB-72) were cultured in Eagle's Minimum Essential Medium (EMEM, Mediatech Media MT-10-009-CV) supplemented with 10% FBS and were incubated at 37 °C under 5% CO₂ and passaged 2-3 times per week according to standard aseptic procedures. SK-MEL-28 cells were started at 200,000 cells/mL in 75 cm² tissue culture flasks and were subcultured when growth reached 550,000 cells/mL by removing old culture media and rinsing the cell layer once with Dulbecco's phosphate buffered saline (DPBS 1X, Mediatech, 21-031-CV), followed by dissociation of cell monolayer with 1X Trypsin-EDTA solution (0.25% (w/v Trypsin/0.53 mM EDTA, ATCC 30-2101). Complete growth medium was added to the cell suspension to allow appropriate aliquots of cells to be transferred to new cell vessels. Complete media was prepared in 150-mL portions as needed by combining EMEM (135 mL) and FBS (15 mL, prealiquoted and heat inactivated) in a 250-mL Millipore vacuum stericup (0.22 μm) and filtering.

Cytotoxicity and photocytotoxicity

Stock solutions of the hexafluorophosphate salts of the iridium complexes were prepared at 5 mM in CH₃CN and kept at -20 °C prior to use. Working dilutions were made by diluting the CH₃CN stock with pH 7.4 Dulbecco's phosphate buffered saline (DPBS). DPBS is a balanced salt solution of 1.47 mM potassium phosphate monobasic, 8.10 mM sodium phosphate dibasic, 2.68 mM potassium chloride, and 0.137 M sodium chloride. CH₃CN was kept at 1% or less in all of the final assay wells.

Cell viability experiments were performed in triplicate in 96-well ultra-low attachment flat bottom microtiter plates (Corning Costar, Acton, MA), where outer wells along the periphery contained 200 μL DPBS (2.68 mM potassium chloride, 1.47 mM potassium phosphate monobasic, 0.137 M sodium chloride, and 8.10 mM sodium phosphate dibasic) to minimize evaporation from sample wells. Cells growing in log phase (HL-60 cells: ~800,000 cells mL⁻¹; SK-MEL-28 cells: ~550,000 cells mL⁻¹) with at least 93% viability were transferred in 50-μL aliquots to inner wells containing warm culture medium (25 μL) and placed in a 37 °C, 5% CO₂ water-jacketed incubator (Thermo Electron Corp., FormaSeries II, Model 3110, HEPA Class 100) for 3 h to equilibrate (and allow for efficient cell attachment in the case of SK-MEL-28 adherent cells). Metals compounds were serially diluted with DPBS and pre-warmed at 37 °C before 25 μL aliquots of the appropriate dilutions were added to cells. PS-treated microplates were incubated at 37 °C under 5% CO₂ for 16 h drug-to-light intervals. Control microplates not receiving a light treatment were kept in the dark in an incubator while light-treated microplates were irradiated under one of the following conditions: visible light (400-700 nm, 34.2 mW·cm⁻²) using a 190 W BenQ MS 510 overhead projector; or red light (625 nm, 29.1 mW·cm⁻²) from an LED array (PhotoDynamic Inc., Mount Uniacke, NS). Irradiation times using these two light sources were approximately 49 and 57 min, respectively, to yield total light doses of 100 J·cm⁻². Both untreated and light-treated microplates were incubated for another 48 h before 10-μL aliquots of prewarmed Alamar Blue reagent (Life Technologies DAL 1025) were added to all sample wells and subsequently incubated for another 15-16 h. Cell viability was determined on

the basis of the ability of the Alamar Blue redox indicator to be metabolically converted to a fluorescent dye only by live cells. Fluorescence was quantified with a Cytofluor 4000 fluorescence microplate reader with the excitation filter set at 530 ± 25 nm and emission filter set at 620 ± 40 nm. EC_{50} values for cytotoxicity (dark) and photocytotoxicity (light) were calculated from sigmoidal fits of the dose–response curves using Graph Pad Prism 6.0 according to Eq 1, where y_i and y_f are the initial and final fluorescence signal intensities. For cells growing in log phase and of the same passage number, EC_{50} values are generally reproducible to within $\pm 25\%$ in the submicromolar regime; $\pm 10\%$ below $10 \mu\text{M}$; and $\pm 5\%$ above $10 \mu\text{M}$. Phototherapeutic indices (PIs), a measure of the therapeutic window, were calculated from the ratio of dark to light EC_{50} values obtained from the dose-response curves.

$$y = y_i + \frac{y_i - y_f}{1 + 10^{(\log EC_{50} - x) \times (\text{Hill slope})}} \quad (1)$$

DNA photocleavage assays

DNA photocleavage experiments were performed according to a general plasmid DNA gel mobility shift assay with $30 \mu\text{L}$ total sample volumes in 0.5 mL microfuge tubes. Transformed pUC19 plasmid ($3 \mu\text{L}$, $>95\%$ form I) was added to $15 \mu\text{L}$ of 5 mM Tris-HCl buffer supplemented with 50 mM NaCl (pH 7.5). Serial dilutions of the Ir(III) compounds were prepared in ddH₂O and added in $7.5 \mu\text{L}$ aliquots to the appropriate tubes to yield final Ir(III) complex concentrations ranging from 1 to $100 \mu\text{M}$. Then, ddH₂O ($4.5 \mu\text{L}$) was added to bring the final assay volumes to $30 \mu\text{L}$. Control samples with no metal complex received $12 \mu\text{L}$ of water. Sample tubes were kept at $37 \text{ }^\circ\text{C}$ in the dark or irradiated. Light treatments employed visible light (14 J cm^{-2}) delivered from a Luzchem LZC-4X photoreactor over the course of 30 min . After treatment, all samples (dark and light) were quenched by the addition of $6 \mu\text{L}$ of gel loading buffer (0.025% bromophenol blue, 40% glycerol). Samples ($11.8 \mu\text{L}$) were loaded onto 1% agarose gels cast with $1\times$ TAE (40 mM Tris-acetate, 1 mM EDTA, pH 8.2) containing ethidium bromide ($0.75 \mu\text{g mL}^{-1}$) and electrophoresed for 30 min at 80 V cm^{-1} in $1\times$ TAE. The bands were visualized using the Gel Doc-It Imaging system (UVP) with Vision Works software and further processed with the GNU Image Maniupulation Program (GIMP).

Confocal microscopy

Sterile glass-bottom Petri dishes (MatTek) were coated with $200 \mu\text{L}$ poly-L-lysine (Ted Pella) in a laminar flow hood under standard aseptic conditions. After a 1 h incubation period at $37 \text{ }^\circ\text{C}$, 5% CO₂ in a water-jacketed incubator (Thermo Electron Corp., Forma Series II, Model 3110, HEPA class 100), the dishes were washed three times with sterile Dulbecco's phosphate buffered saline (DPBS 1 \times , Mediatech, 21-031-CV) containing 2.68 mM potassium chloride, 1.47 mM potassium phosphate monobasic, 0.137 M sodium chloride, and 8.10 mM sodium phosphate dibasic, pH 7.4, and were left to dry uncovered at room temperature for approximately 15 min .

SK-MEL-28 malignant melanoma cells (ATCC HTB-72) were then transferred in aliquots of 500 μL (approximately 100,000 cells) to the poly-Llysine-coated glass bottom Petri dishes and were allowed to adhere for 2 h in a 37 °C, 5% CO_2 water-jacketed incubator. Metal compound (500 μL of a 50 μM solution in sterile PBS prewarmed to 37 °C) was added to sample dishes (destined to receive either a dark or light treatment), which were returned to the incubator for 15 min prior to further treatment; control dishes that did not contain the metal compound were also prepared. Light-treated samples were irradiated with visible light for 25 min from a 190 W BenQ MS 510 overhead projector (400–700 nm, power density = 33.1 mW cm^{-2} , total light dose $\approx 50 \text{ J cm}^{-2}$). Dark samples were covered with foil and placed in a drawer for the same amount of time. Cells were then imaged at 15 min post-treatment using a Carl Zeiss LSM 510 laser scanning confocal microscope with a 60 \times oil objective lens. Excitation was delivered at 458/488 nm from an argon–krypton laser, and signals were acquired through a 475 nm long-pass filter. Pinhole diameters for all the treatments were 100 μm . The images were collected and analyzed using the Zeiss LSM Image Browser Version 4.2.0.121 software (Carl Zeiss Inc.).

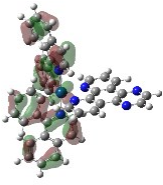
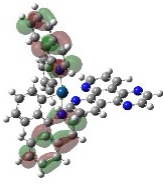
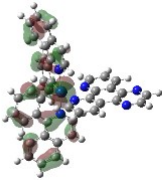
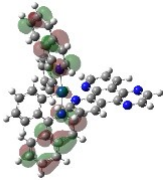
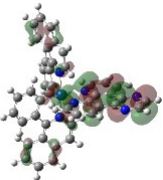
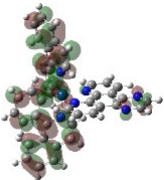
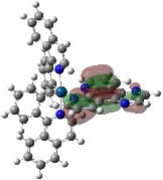
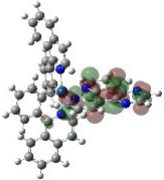
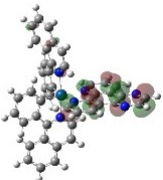
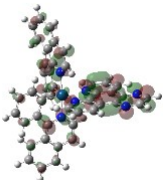
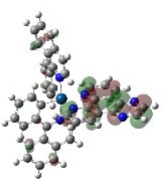
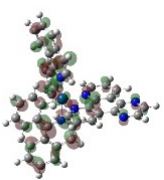
References

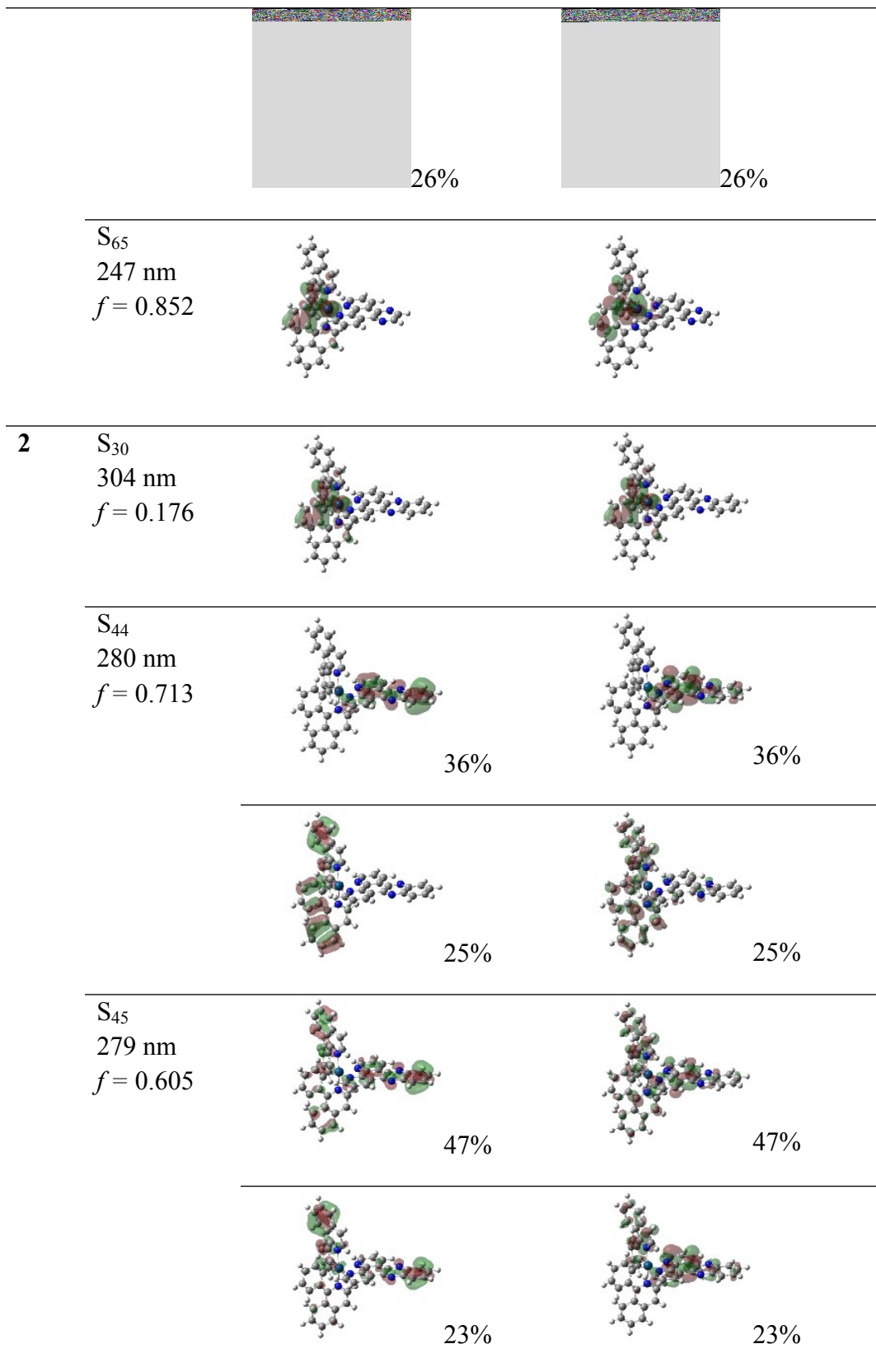
- 1 H.-Y. Chen, C.-H. Yang, Y. Chi, Y.-M. Cheng, Y.-S. Yeh, P.-T. Chou, H.-Y. Hsieh, C.-S. Liu, S.-M. Peng, G.-H. Lee, *Can. J. Chem.* **2006**, *84*, 309-318.
- 2 a) Z. Molphy, A. Prisecaru, C. Slator, N. Barron, M. McCann, J. Colleran, D. Chandran, N. Gathergood, A. Kellett, *Inorg. Chem.* **2014**, *53*, 5392-5404; b) F. Miomandre, S. Stancheva, J.-F. Audibert, A. Brosseau, R. B. Pansu, M. Lepeltier, C. R. Mayer, *J. Phys. Chem. C* **2013**, *117*, 12806-12814.
- 3 G. A. Crosby, J. N. Demas, *J. Phys. Chem.* **1971**, *75*, 991-1024.
- 4 K. Suzuki, A. Kobayashi, S. Kaneko, K. Takehira, T. Yoshihara, H. Ishida, Y. Shiina, S. Oishi, S. Tobita, *Phys. Chem. Chem. Phys.* **2009**, *11*, 9850-9860.
- 5 J. P. Perdew, *Phys. Rev. B* **1986**, *33*, 8822.
- 6 C. V. Kumar, L. Qin, P. K. Das, *J. Chem. Soc. Faraday Trans.* **1984**, *80*, 783-793.
- 7 P. A. Firey, W. E. Ford, J. R. Sounik, M. E. Kenney, M. A. Rodgers, *J. Am. Chem. Soc.* **1988**, *110*, 7626-7630.
- 8 F. Guo, W. Sun, Y. Liu, K. Schanze, *Inorg. Chem.* **2005**, *44*, 4055-4065.
- 9 M. J. Frisch, G. W. Trucks, H. B. Schlegel, G. E. Scuseria, M. A. Robb, J. R. Cheeseman, G. Scalmani, V. Barone, B. Mennucci, G. A. Petersson, H. Nakatsuji, M. Caricato, X. Li, H. P. Hratchian, A. F. Izmaylov, J. Bloino, G. Zheng, J. L. Sonnenberg, M. Hada, M. Ehara, K. Toyota, R. Fukuda, J. Hasegawa, M. Ishida, T. Nakajima, Y. Honda, O. Kitao, H. Nakai, T.

Vreven, Jr., J. A. Montgomery, J. E. Peralta, F. Ogliaro, M. Bearpark, J. J. Heyd, E. Brothers, K. N. Kudin, V. N. Staroverov, R. Kobayashi, J. Normand, K. Raghavachari, A. Rendell, J. C. Burant, S. S. Iyengar, J. Tomasi, M. Cossi, N. Rega, N. J. Millam, M. Klene, J. E. Knox, J. B. Cross, V. Bakken, C. Adamo, J. Jaramillo, R. Gomperts, R. E. Stratmann, O. Yazyev, A. J. Austin, R. Cammi, C. Pomelli, J. W. Ochterski, R. L. Martin, K. Morokuma, V. G. Zakrzewski, G. A. Voth, P. Salvador, J. J. Dannenberg, S. Dapprich, A. D. Daniels, Ö. Farkas, J. B. Foresman, J. V. Ortiz, J. Cioslowski, D. J. Fox, Gaussian 09, Revision A.1, Gaussian Inc., Wallingford, CT, USA, 2009.

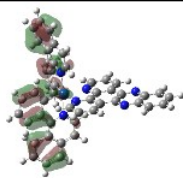
- 10 J. P. Perdew, M. Ernzerhof, K. Burke, *J. Chem. Phys.* **1996**, *105*, 9982-9985.
- 11 a) C. Pei, P. Cui, C. McCleese, S. Kilina, C. Burda, W. Sun, *Dalton Trans.* **2015**, *44*, 2176-2190; b) R. Liu, N. Dandu, J. Chen, Y. Li, Z. Li, S. Liu, C. Wang, S. Kilina, B. Kohler, W. Sun, *J. Phys. Chem. C* **2014**, *118*, 23233-23246; c) Y. Li, N. Dandu, R. Liu, Z. Li, S. Kilina, W. Sun, *J. Phys. Chem. C* **2014**, *118* (12), 6372-6384; d) Y. Li, N. Dandu, R. Liu, L. Hu, S. Kilina, W. Sun, *ACS Appl. Mater. Interfaces.* **2013**, *5* (14), 6556-6570; e) Y. Li, N. Dandu, R. Liu, S. Kilina, W. Sun, *Dalton Trans.* **2014**, *43* (4), 1724-1735; f) Z. Li, P. Cui, C. Wang, S. Kilina, W. Sun, *J. Phys. Chem. C* **2014**, *118*(49), 28764-28775.
- 12 a) P. J. Hay, W. R. Wadt, *J. Chem. Phys* **1985**, *82*, 270-283; b) R. Krishnan, J. S. Binkley, R. Seeger, J. A. Pople, *J. Chem. Phys* **1980**, *72*, 650-654; c) L. E. Roy, G. Scalmani, R. Kobayashi, E. R. Batista, *Dalton Trans.* **2009**, 6719-6721; d) M. J. G. Peach, P. Benfield, T. Helgaker, D. J. Tozer, *J. Chem. Phys* **2008**, *128*, 044118; e) A. Vlček Jr, S. Zláliš, *Coord. Chem. Rev.* **2007**, *251*, 258-287.
- 13 a) T. Yanai, D. P. Tew, N. C. Handy, *Chem. Phys. Lett.* **2004**, *393*, 51-57; b) V. Barone, M. Cossi, J. Tomasi, *J. Comput. Chem.* **1998**, *19*, 404-417.
- 14 R. L. Martin, *J. Chem. Phys* **2003**, *118*, 4775-4777.
- 15 R. Dennington, II; Keith, T.; Millam, J., *GaussView; Semichem Inc.: Shawnee Mission, KS* **2007**.

Table S1 Natural transition orbitals (NTOs) representing transitions contributing to the absorption bands below 320 nm for **1-3** and below 350 nm for **4-6** in CH₃CN.

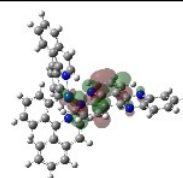
	S_n	Hole	Electron
1	S ₄₂ 273 nm $f = 0.567$	 42%	 42%
		 29%	 29%
	S ₆₁ 252 nm $f = 0.166$		
	S ₆₂ 252 nm $f = 0.655$	 47%	 47%
		 38%	 38%
	S ₆₃ 252 nm $f = 0.218$	 61%	 61%



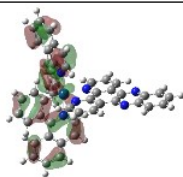
S₄₇
275 nm
 $f = 0.300$



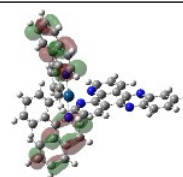
34%



34%

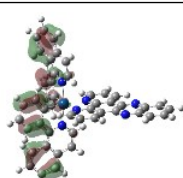


29%

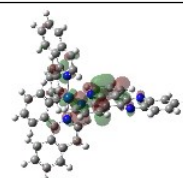


29%

S₄₈
273 nm
 $f = 0.275$

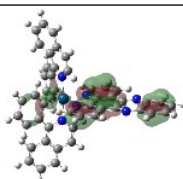


50%

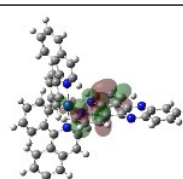


50%

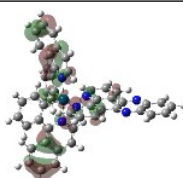
S₆₅
254 nm
 $f = 0.160$



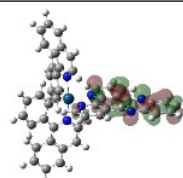
24%



24%

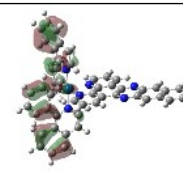


22%

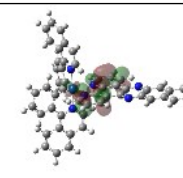


22%

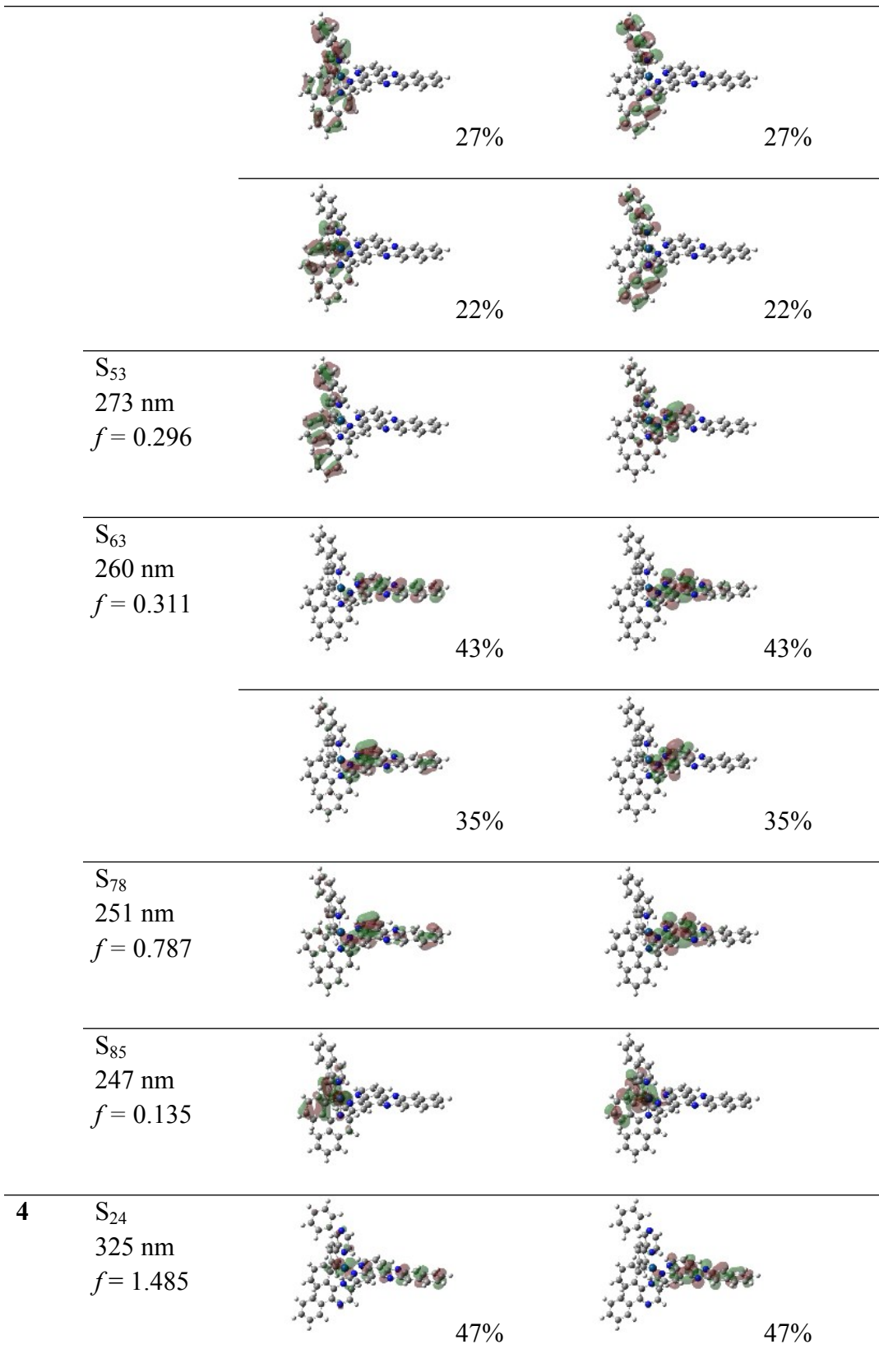
3 S₅₂
275 nm
 $f = 0.242$

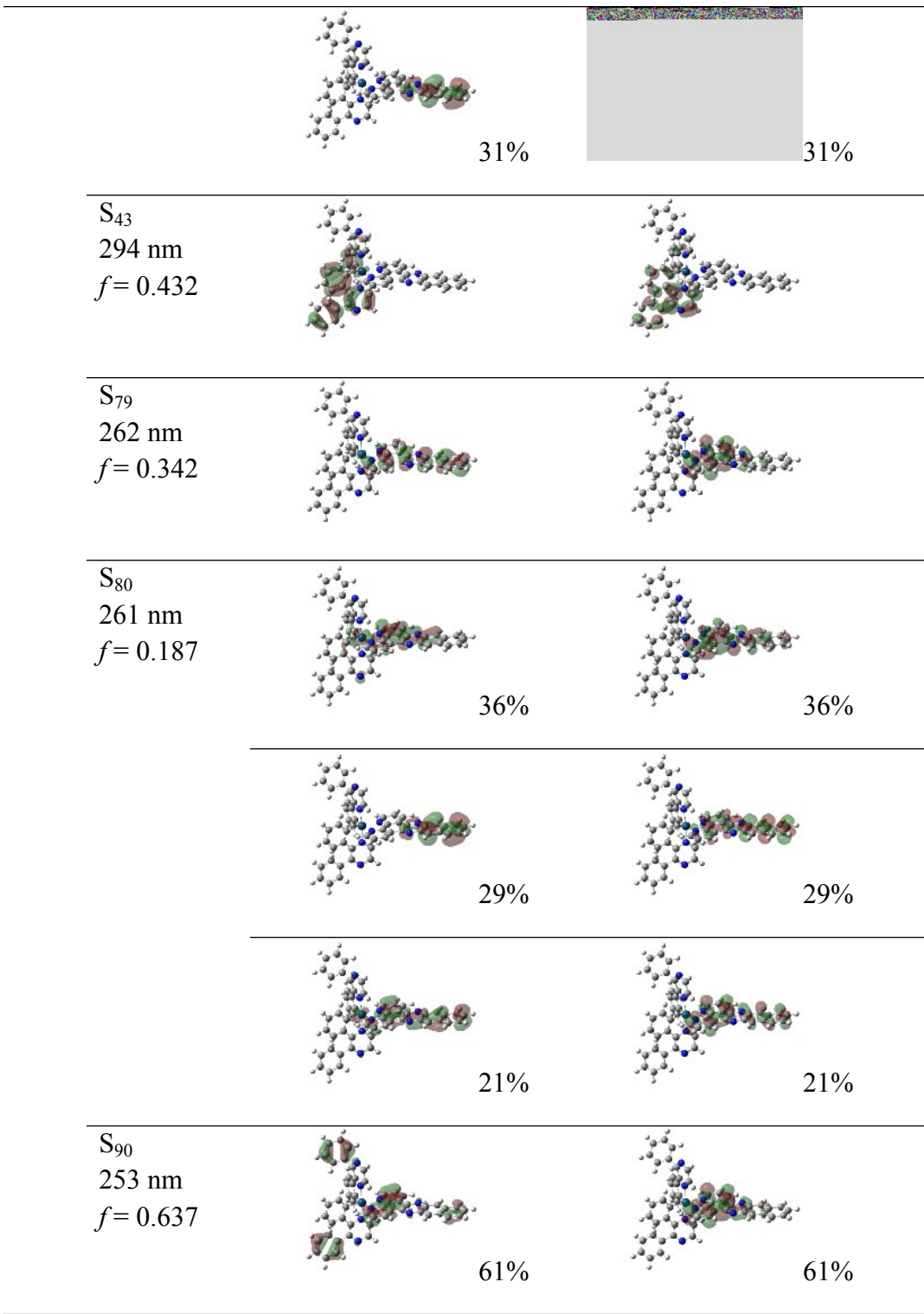


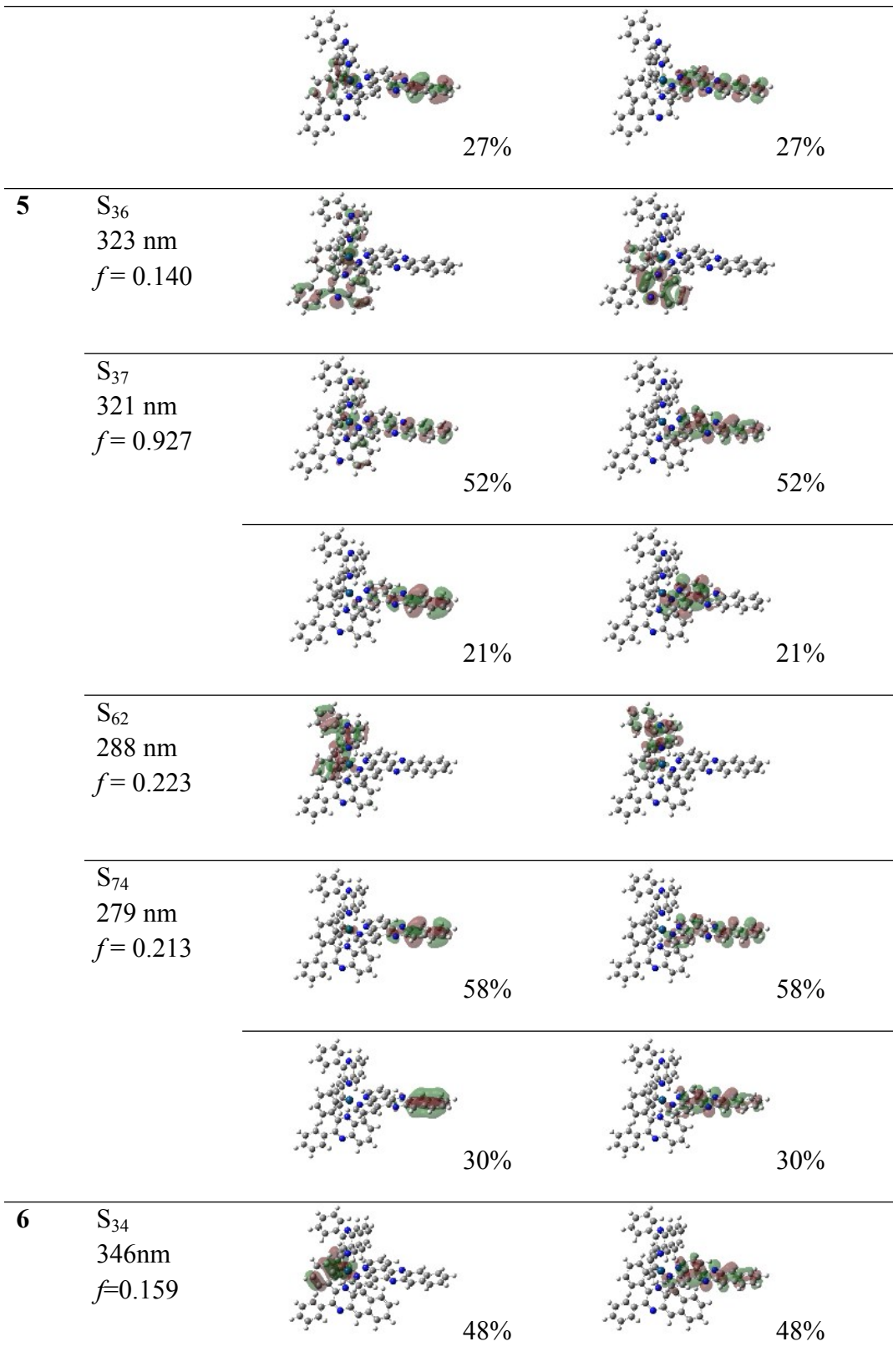
37%

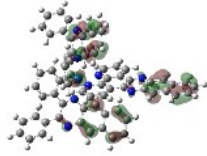


37%

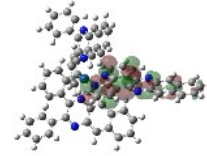






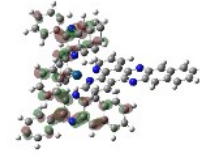
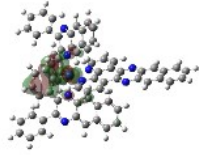


30%

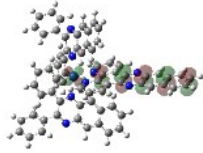


30%

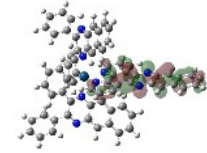
S₃₈
337 nm
 $f = 0.245$



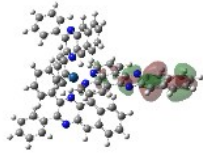
S₄₃
326 nm
 $f = 1.435$



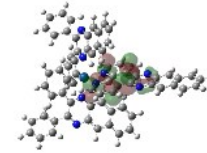
52%



52%

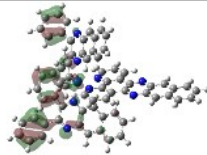


41%

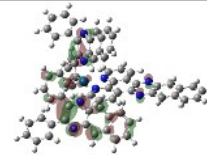


41%

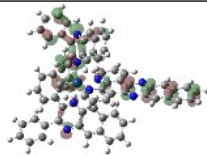
S₅₆
307 nm
 $f = 0.221$



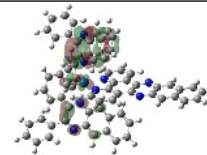
37%



37%



26%



26%

S₅₇
305 nm
 $f = 0.420$

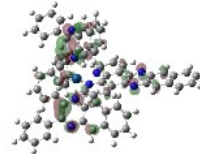
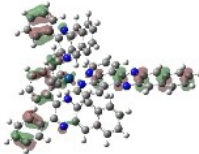
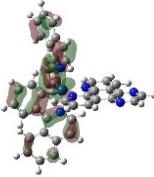
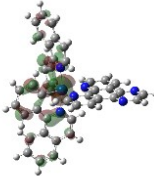
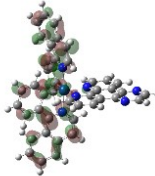
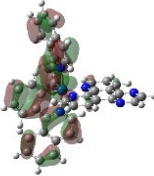
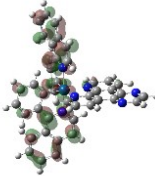
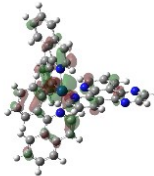
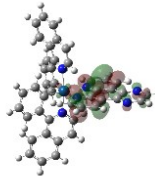
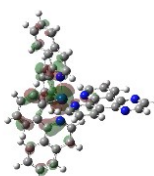
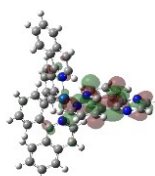
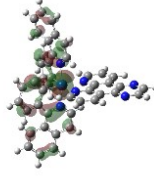
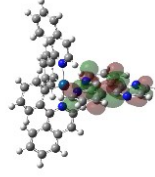
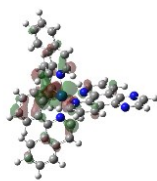
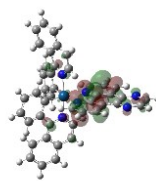


Table S2 Natural transition orbitals (NTOs) representing transitions contributing to the absorption bands in 320-400 nm for **1-3** and 350-450 nm for **4-6** in CH₃CN.

	S_n	Hole	Electron
1	S_6 384 nm $f = 0.057$		
	S_9 354 nm $f = 0.080$		
	S_{12} 345 nm $f = 0.090$		
	S_{13} 343 nm $f = 0.084$		
			58%
			
		41%	41%
	S_{15} 338 nm $f = 0.096$		
		60%	60%

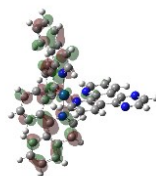
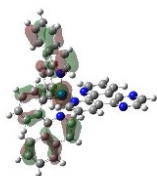


30%

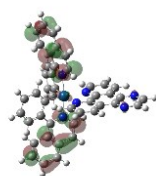
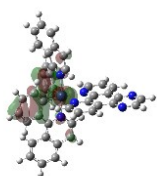


30%

S₂₁
320 nm
 $f = 0.268$

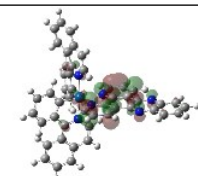
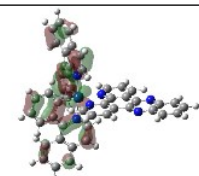


S₂₉
303 nm
 $f = 0.189$

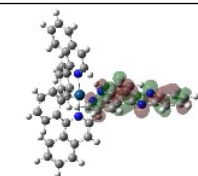
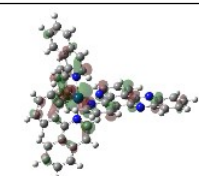


2

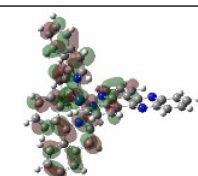
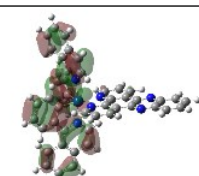
S₈
374 nm
 $f = 0.098$



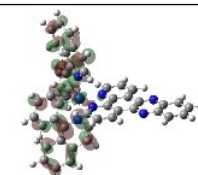
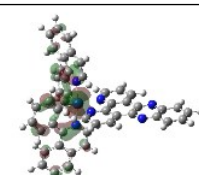
S₁₁
361 nm
 $f = 0.087$

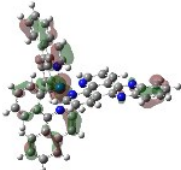
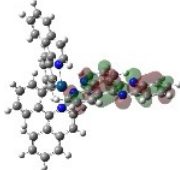
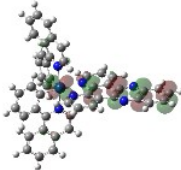
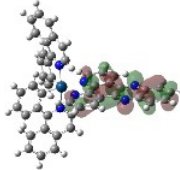
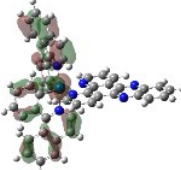
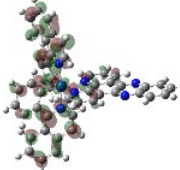
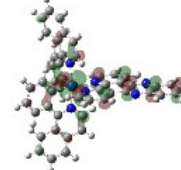
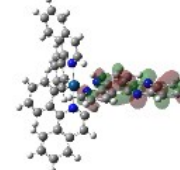
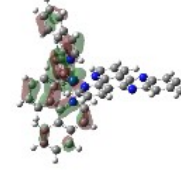
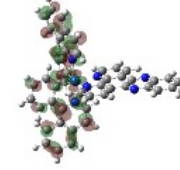
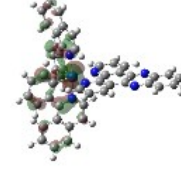
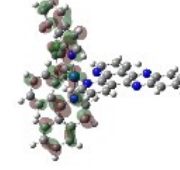
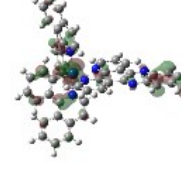
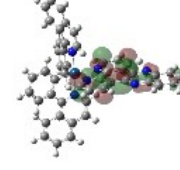


S₁₂
359 nm
 $f = 0.068$

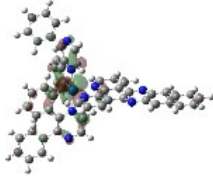
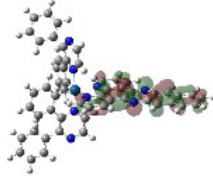
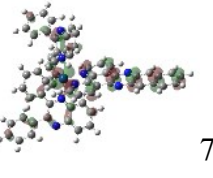
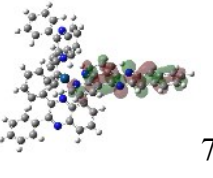
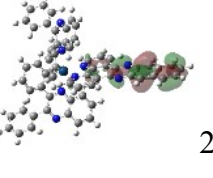
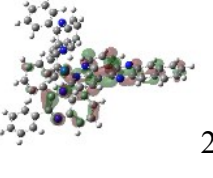
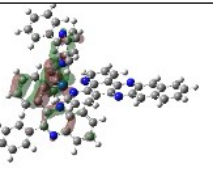
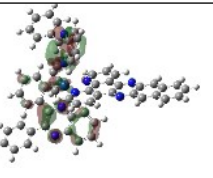
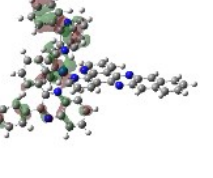
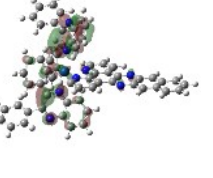
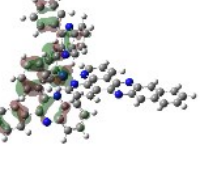
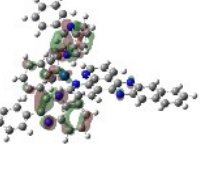
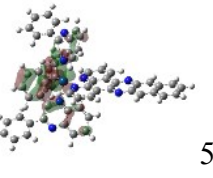
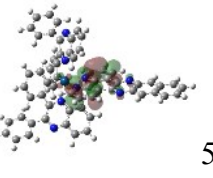


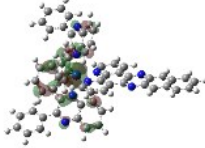
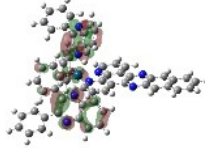
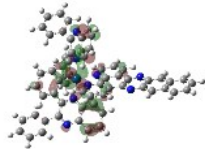
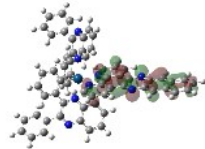
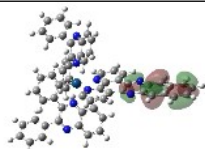
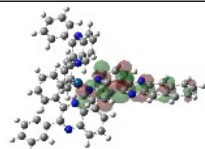
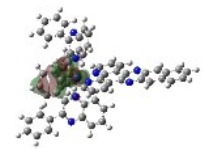
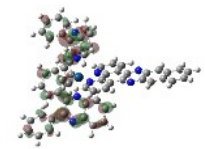
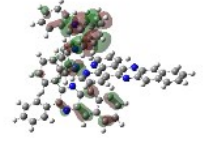
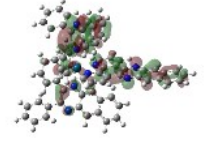
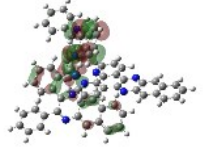
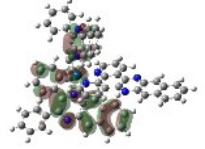
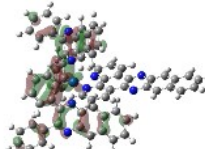
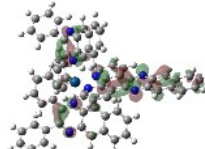
S₁₄
353 nm
 $f = 0.088$



	S_{15} 351 nm $f = 0.014$		
	S_{23} 322 nm $f = 0.146$		
	S_{24} 319 nm $f = 0.243$		
3	S_9 387 nm $f = 0.230$		
	S_{19} 345 nm $f = 0.117$		
	S_{20} 337 nm $f = 0.291$		
	S_{25} 325 nm $f = 0.778$		

	S_{26} 323 nm $f = 0.580$		
	S_{27} 322 nm $f = 0.253$		
	S_{28} 320 nm $f = 0.223$		
	S_{36} 305 nm $f = 0.191$		
4	S_4 427 nm $f = 0.050$		
	S_{10} 380 nm $f = 0.184$		
	S_{14} 354 nm $f = 0.217$		
		60%	60%

			
		23%	23%
5	S_9 386 nm $f = 0.079$		
		73%	73%
			
		25%	25%
	S_{10} 384 nm $f = 0.119$		
	S_{18} 367 nm $f = 0.103$		
	S_{19} 366 nm $f = 0.132$		
	S_{22} 352 nm $f = 0.129$		
		56%	56%

			29		29%
	%				
S_{26} 341 nm $f = 0.598$			44		44%
	%				
			28		28%
	%				
S_{28} 340 nm $f = 0.204$					
6	S_8 458 nm $f = 0.060$				
	S_{10} 428 nm $f = 0.012$				
	S_{15} 397 nm $f = 0.134$				

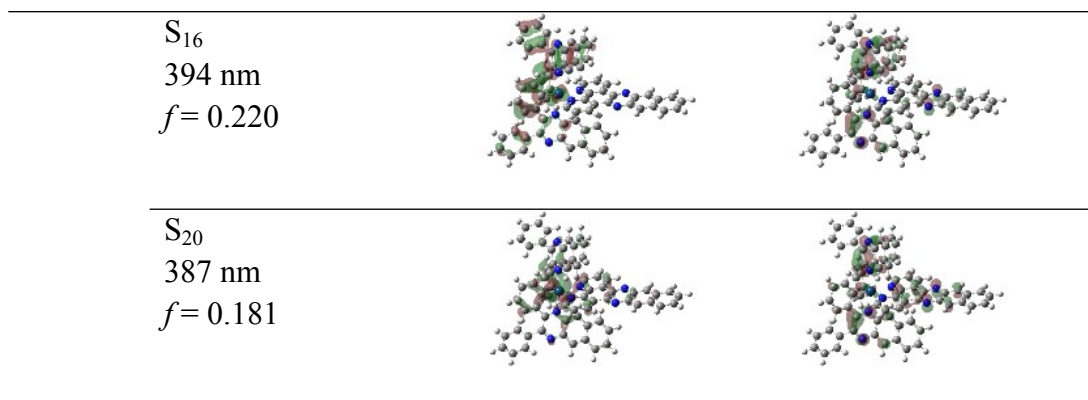


Table S3 Characteristics of molecular orbitals for the first five HOMOs and LUMOs of complexes **1-6**.

MO	1	2	3	4	5	6
LUMO+4	piq/ $d(\text{Ir})$	piq/ $d(\text{Ir})$	dppz(π^*)/piq	dpp(π^*)/ $d_{z^2}(\text{Ir})$	dppn(π^*)	dppn(π^*)
LUMO+3	$d(\text{Ir})$ /piq	dpq(π^*)	delocalized	dppn(π^*)	dppn(π^*)	dppn(π^*)
LUMO+2	dpq(π^*)	piq/ $d(\text{Ir})$	piq/ $d(\text{Ir})$	dpp(π^*)/ $d(\text{Ir})$	dpqx(π^*)-N/ $d(\text{Ir})$	dpbq(π^*)/ $d(\text{Ir})$
LUMO+1	dpq(π^*)	dppz(π^*)	dppz(π^*)/ $d(\text{Ir})$	dppn(π^*)	dpqx(π^*)/ $d(\text{Ir})$	dpbq(π^*)/ $d(\text{Ir})$
LUMO	dpq(π^*)	dppz(π^*)	dppz(π^*)	dppn(π^*)	dppn(π^*)	dppn(π^*)
HOMO	$d(\text{Ir})$ /Ph(π)	$d(\text{Ir})$ /Ph(π)	$d(\text{Ir})$ /Ph(π)	Ph(π)/ $d(\text{Ir})$	$d(\text{Ir})$ /dpqx(π)-N	$d(\text{Ir})$ /dpbq(π)
HOMO-1	piq(π)/ d	Piq(π)/ $d(\text{Ir})$	dppn(π)	dpp(π)	dppn(π)	dppn(π)
HOMO-2	$d_{z^2}(\text{Ir})$ /piq(π)	$d_{z^2}(\text{Ir})$ /piq(π)	piq(π)/ d	dpp(π)/ $d(\text{Ir})$	dpqx(π)/ $d(\text{Ir})$	dpbq(π)-N/ $d(\text{Ir})$
HOMO-3	$d(\text{Ir})$ /Ph(π)	$d(\text{Ir})$ /Ph(π)	$d(\text{Ir})$ /piq(π)	$d_{z^2}(\text{Ir})$ /dpp(π)	$d(\text{Ir})$ /dpqx(π)	dpbq(π)/ $d(\text{Ir})$
HOMO-4	d_{z^2} /piq(π)	d_{z^2} /piq(π)	$d(\text{Ir})$ /Ph(π)	dpp(π)	dpqx(π)/ $d(\text{Ir})$	dpbq(π)

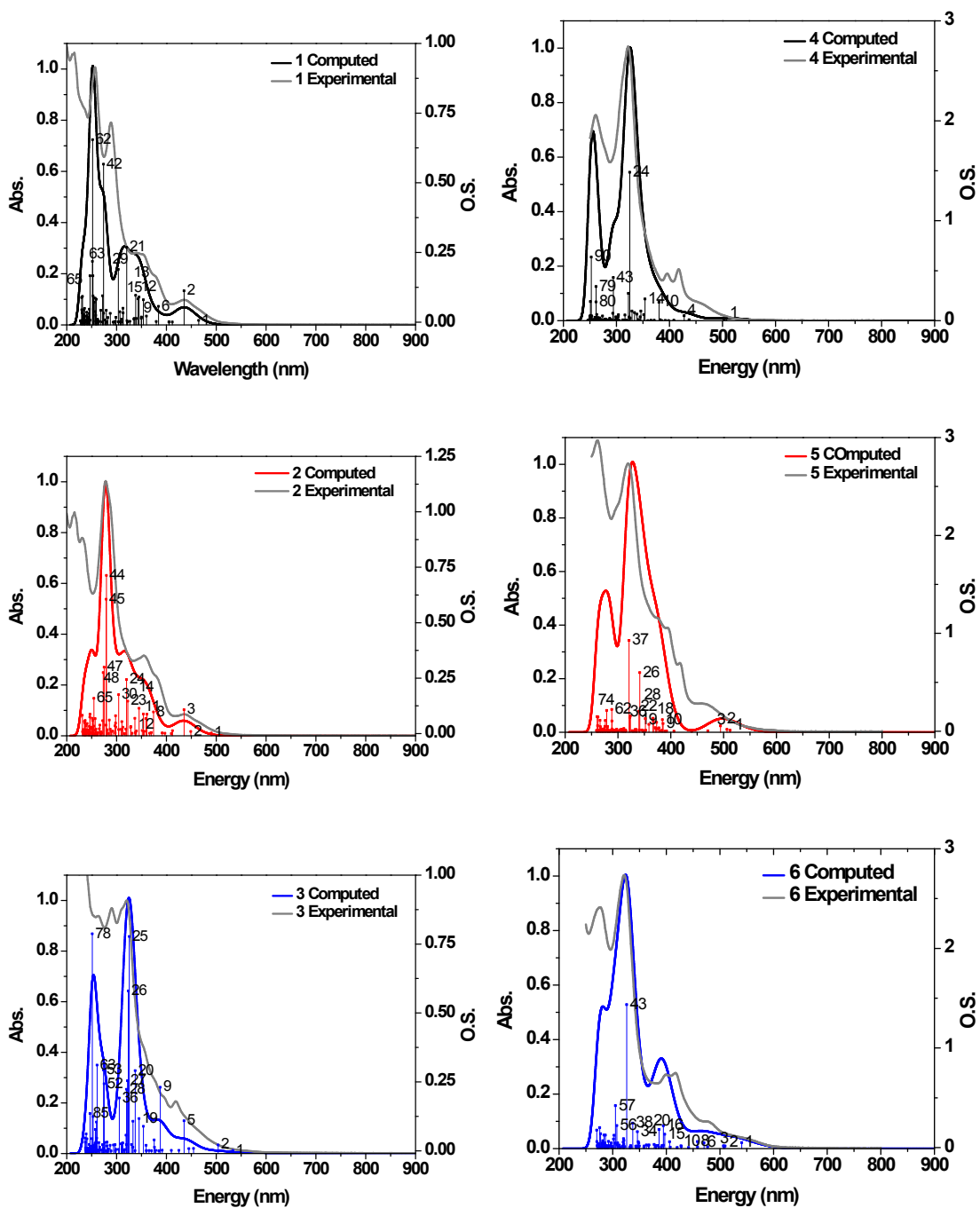


Fig. S1 Comparison of normalized experimental versus computational UV-vis absorption spectra of complexes 1-6 in CH₃CN.

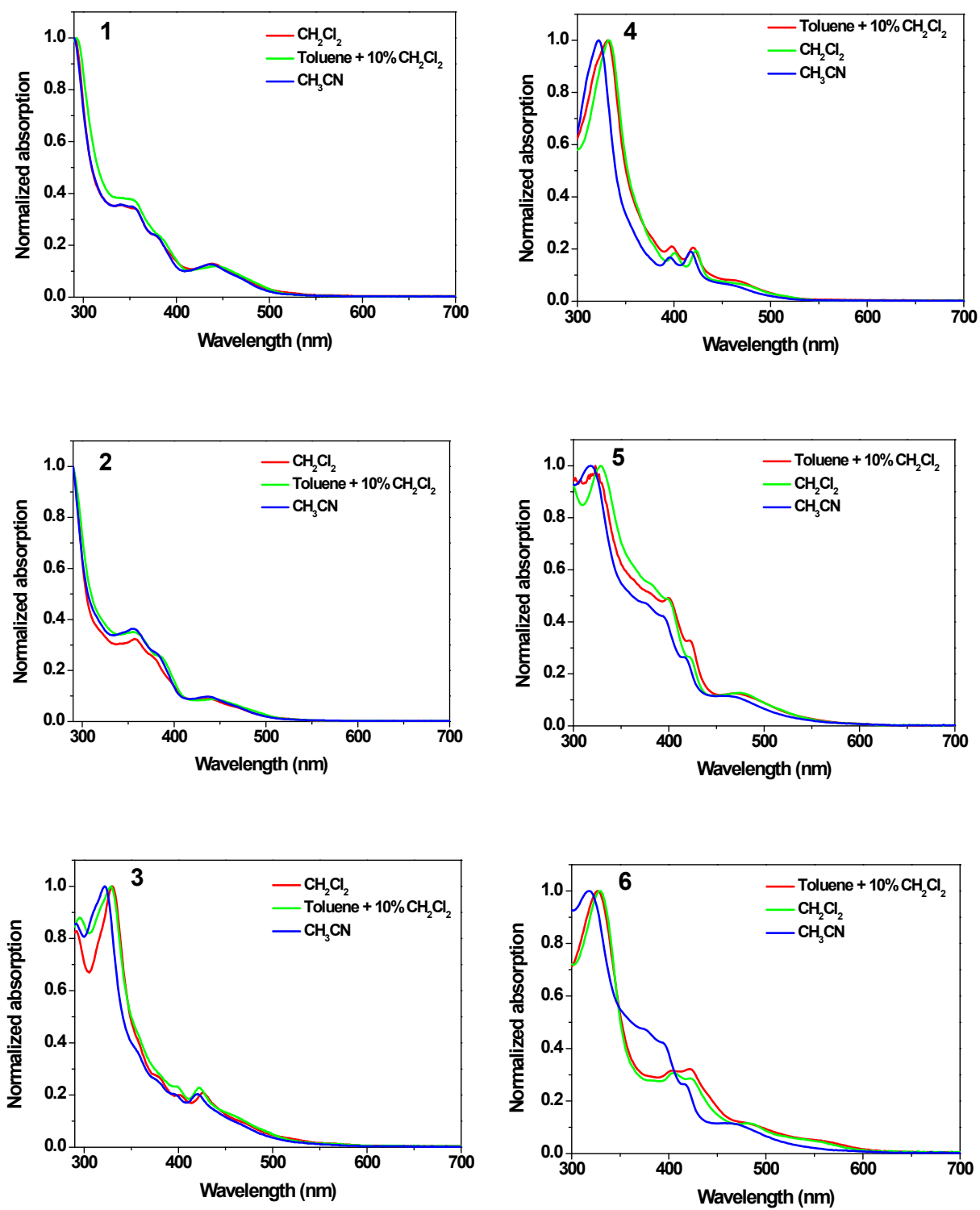


Fig. S2 Normalized UV-vis absorption spectra of complexes 1-6 in different solvents.

Table S4 Emission characteristics of complexes **1-6** in different deoxygenated solvents.

	λ_{em}/nm (τ_{em}/ns ; Φ_{em})			
	Hexane (+10% CH ₂ Cl ₂)	CH ₂ Cl ₂	Toluene (+10% CH ₂ Cl ₂)	CH ₃ CN
1	587 (2640; 0.087)	585 (2930; 0.33)	591 (2660; 0.25)	588 (2980; 0.22)
2	588 (2650; 0.033)	586 (2590; 0.30)	590 (2620; 0.25)	590 (400; 0.034)
3	589 (2480; 0.007)	587 (3000; 0.034)	593 (2540; 0.027)	591 (2690; 0.026)
4	546 (2220; 0.032)	551 (2230; 0.044)	552 (2250; 0.057)	554 (2520; 0.015)
5	625 (2390; 0.015)	625 (2430; 0.136)	632 (1610; 0.048)	629 (2390; 0.083)
6	613 (-; -) ^a	621 (450; -) ^a	631 (1170; -) ^a	558 (60; -), 774 (-; -) ^a

^aToo weak to be measured.

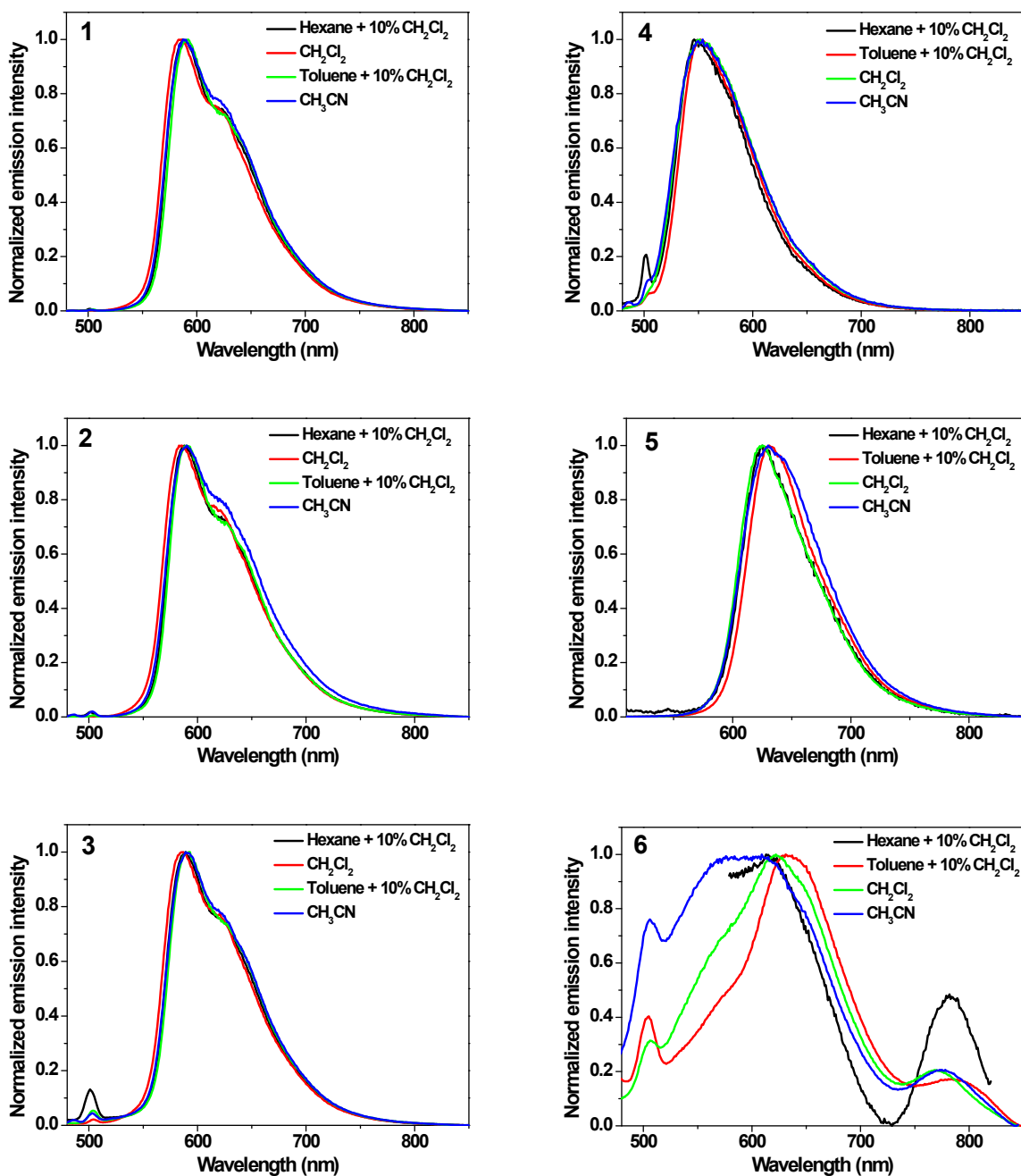


Fig. S3 Normalized emission spectra of complexes **1-6** in different deoxygenated solvents at room temperature. $\lambda_{\text{ex}} = 436$ nm and $A_{436} = 0.08$ in a 1-cm cuvette.

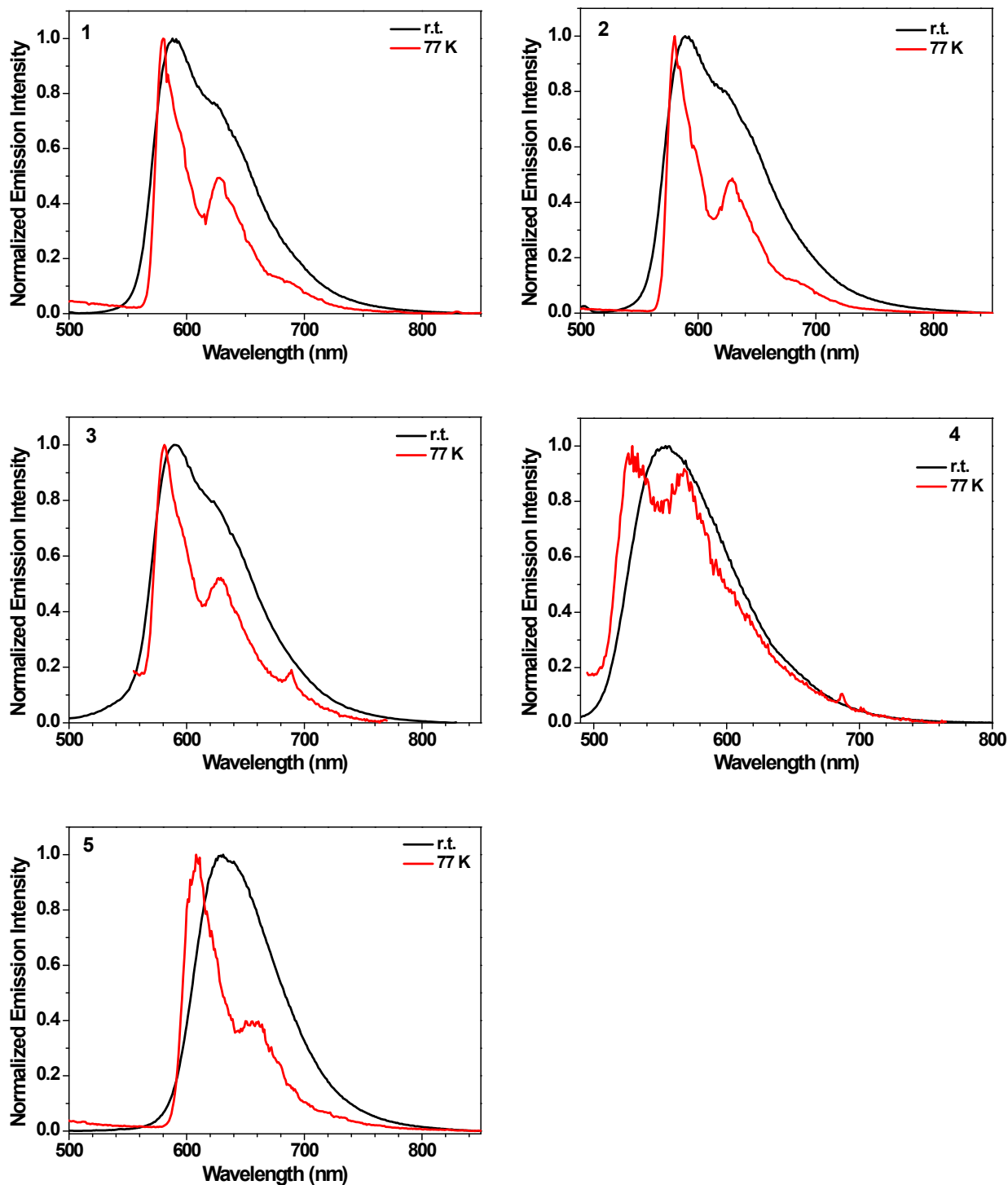


Fig. S4 Normalized emission spectra of complexes **1-6** in deoxygenated CH_3CN solution at r.t. and in BuCN glassy matrix at 77 K. λ_{ex} was 435 nm for **1**, 436 nm for **2**, 419 nm for **3**, 418 nm for **4**, and 466 nm for **5**. The emission of **6** at 77 K was unable to be detected due to the very weak signal and the poor quality of the glassy matrix.

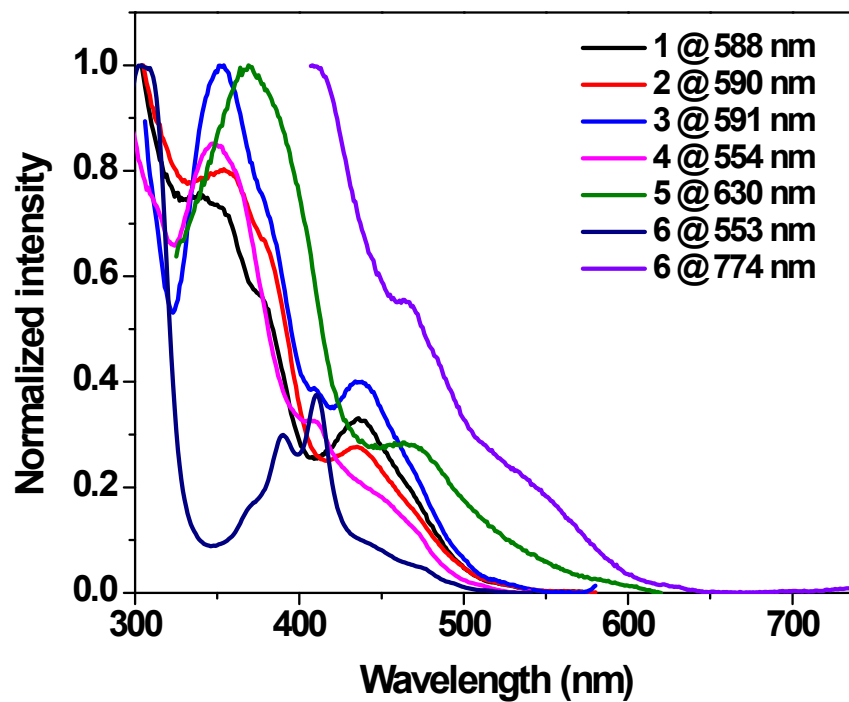


Fig. S5 Normalized excitation spectra of complexes **1-6** in deoxygenated CH₃CN monitored at their respective emission maxima.

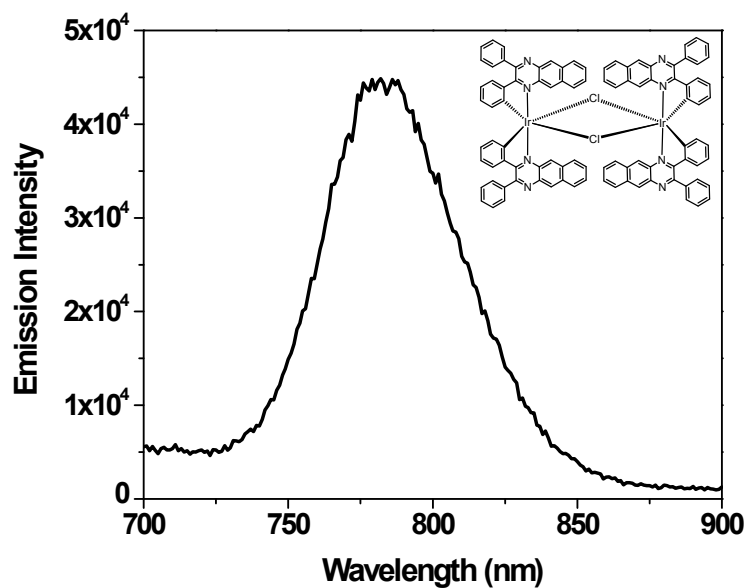
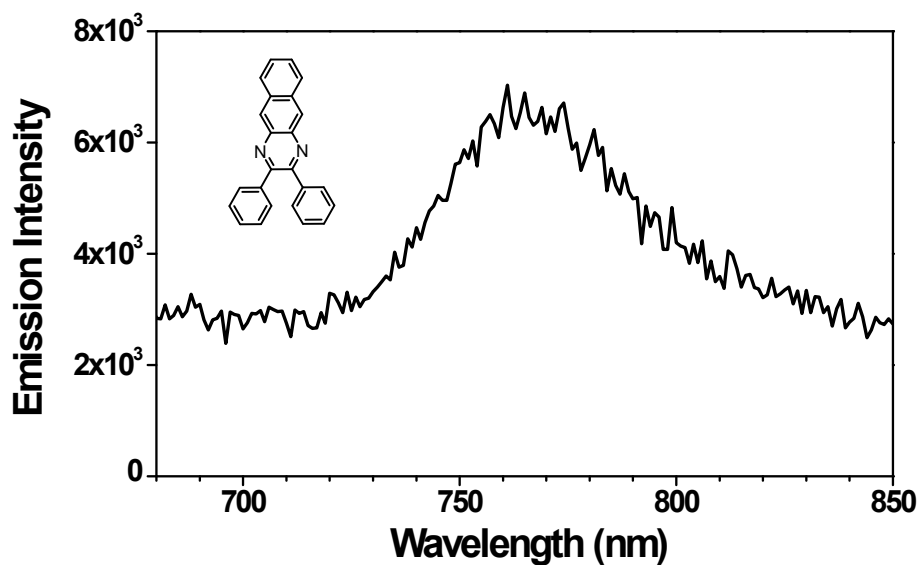


Fig. S6 Phosphorescence spectra of dpbq ligand with addition of 2 eq. $(\text{C}_2\text{H}_5)_4\text{N}^+\text{I}^-$ ($\lambda_{\text{ex}} = 430$ nm) and the $[(\text{dpbq})_2\text{IrCl}]_2$ dimer ($\lambda_{\text{ex}} = 504$ nm) in degassed CH_2Cl_2 solutions. $c = 1 \times 10^{-5}$ mol/L.

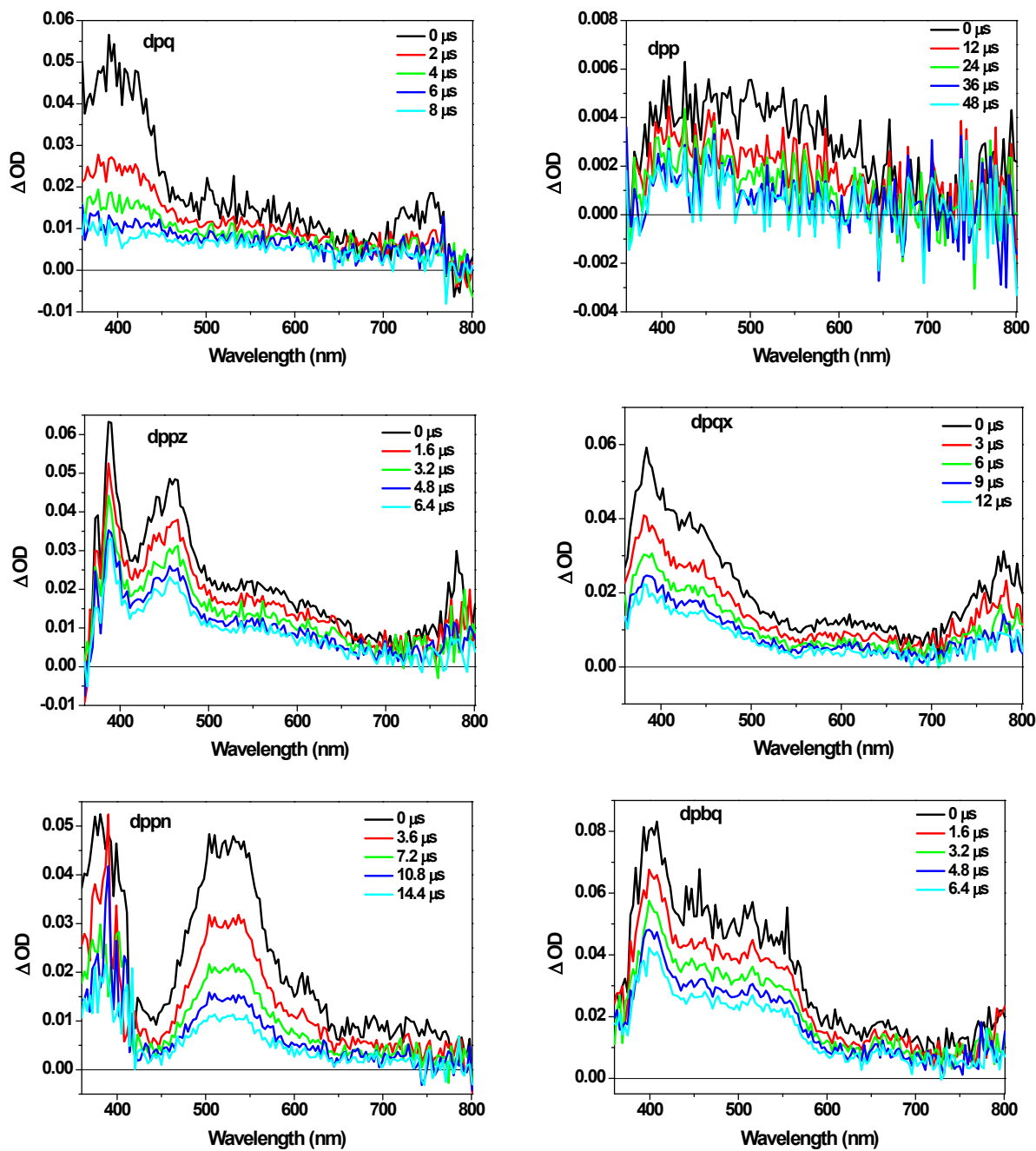


Fig. S7 Time-resolved ns transient absorption spectra of ligands in deoxygenated CH₃CN. $\lambda_{\text{ex}} = 355 \text{ nm}$, $A_{355} = 0.4$ in a 1-cm cuvette.

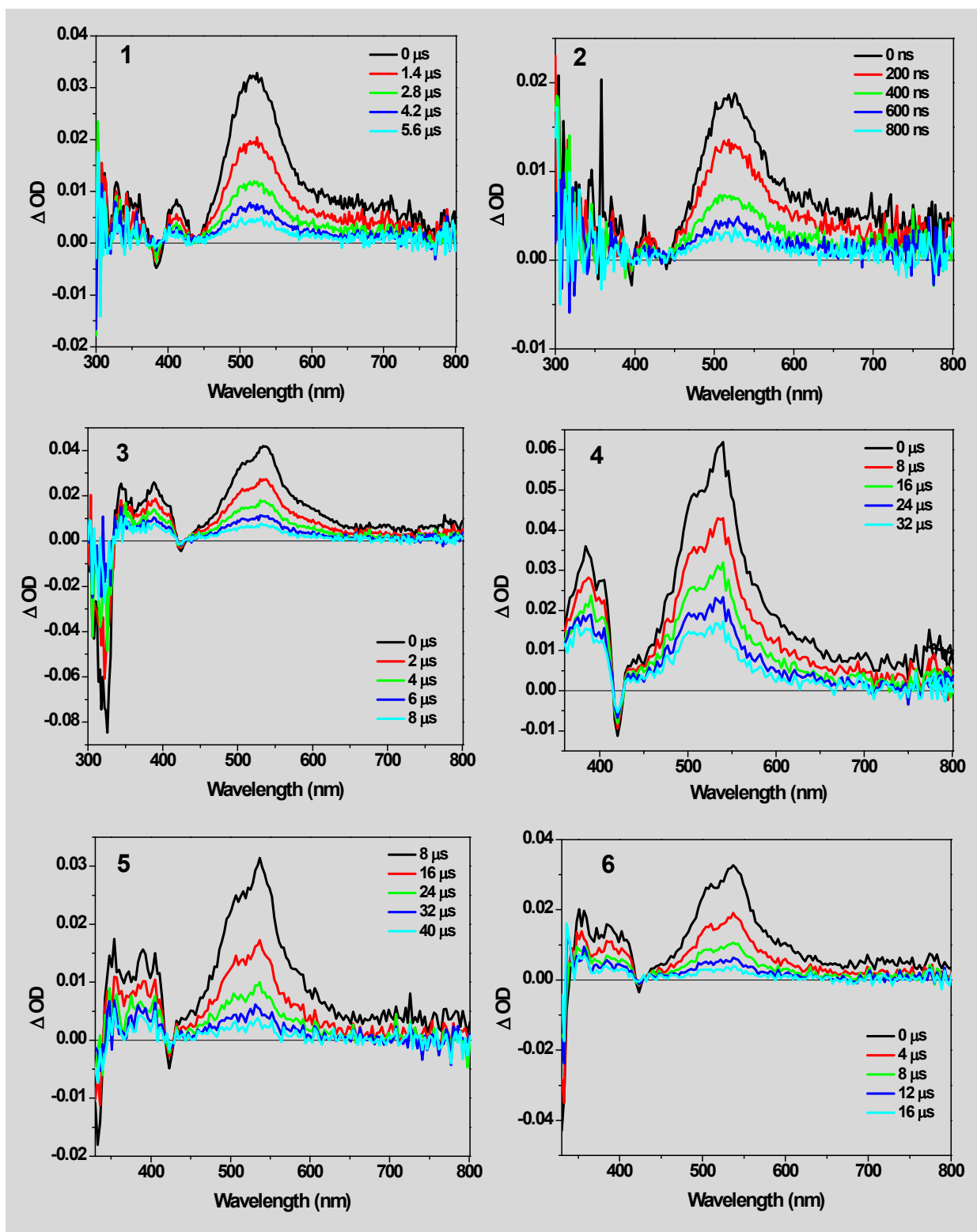


Fig. S8 Time-resolved ns transient absorption spectra of complexes 1-6 in deoxygenated CH_3CN . $\lambda_{\text{ex}} = 355 \text{ nm}$, $A_{355} = 0.4$ in a 1-cm cuvette.

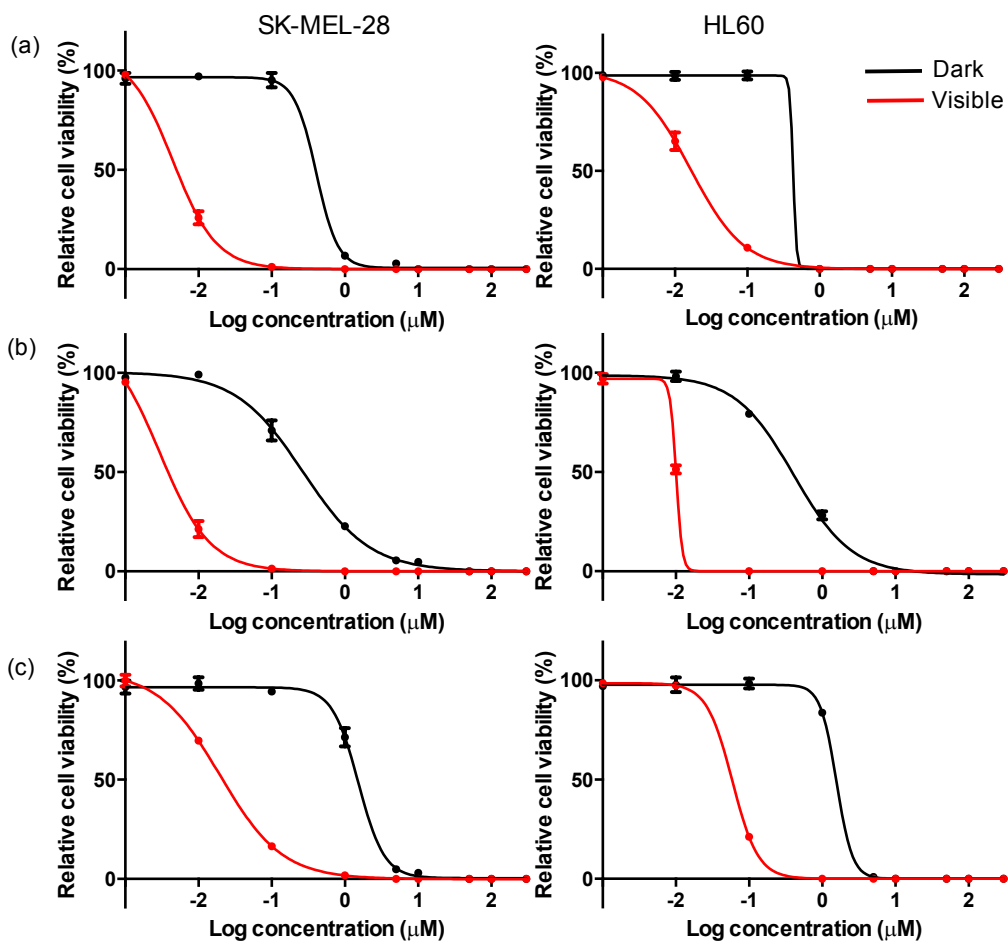


Fig. S9 In vitro dose-response curves for complexes **1** (a), **2** (b) and **3** (c) in SK-MEL-28 (left column) and HL60 cells (right column) in the dark (black) or with a visible light activation (red).

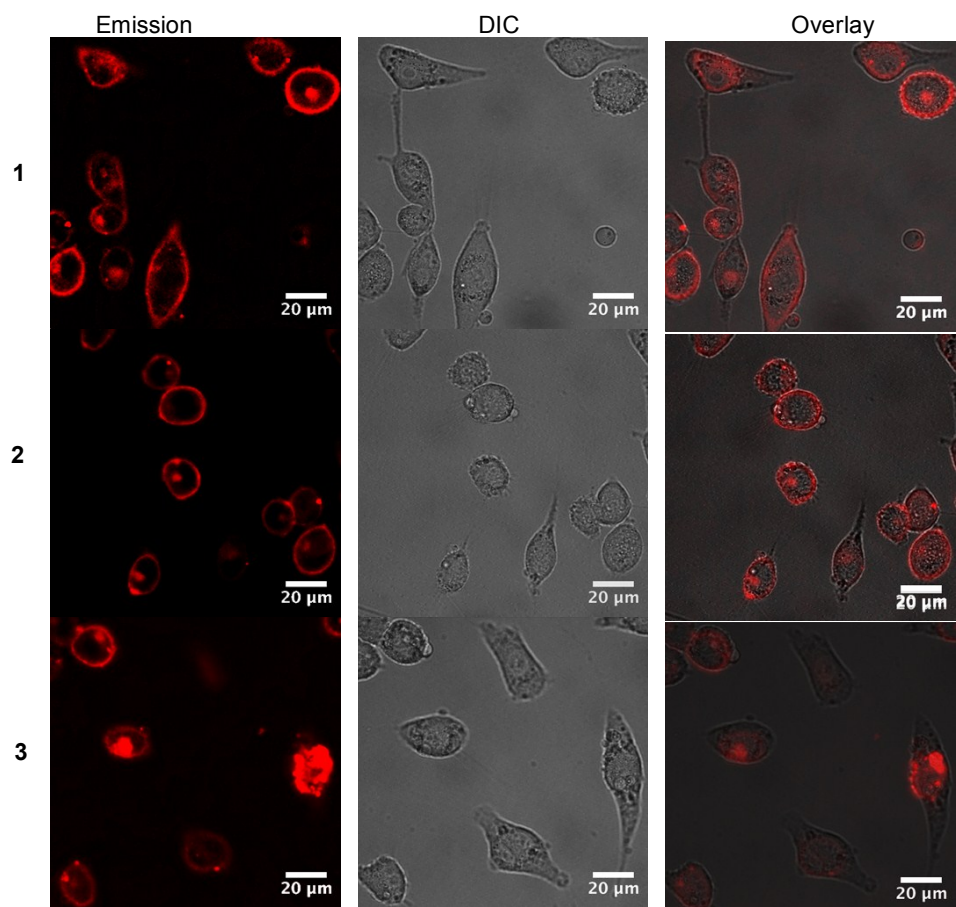


Fig. S10 Confocal luminescence images of SK-MEL-28 cells dosed with 50 μM complex **1** or **2** and **3** in the dark.

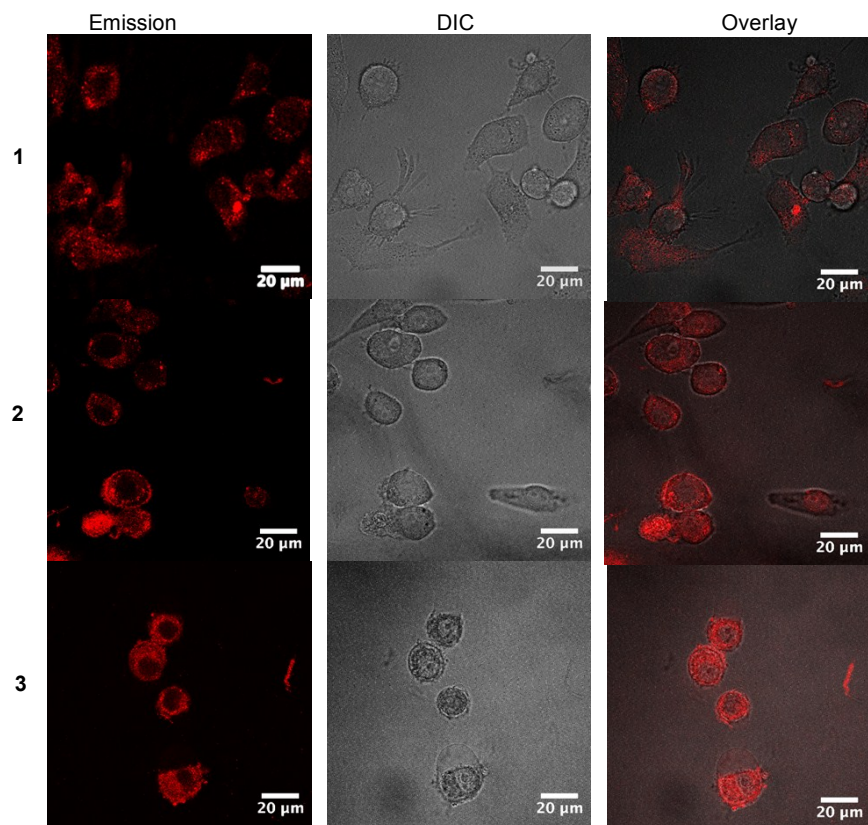


Fig. S11 Confocal luminescence images of SK-MEL-28 cells dosed with 50 μM complex **1** or **2** and **3** activated by visible light (50 J cm^{-2}).

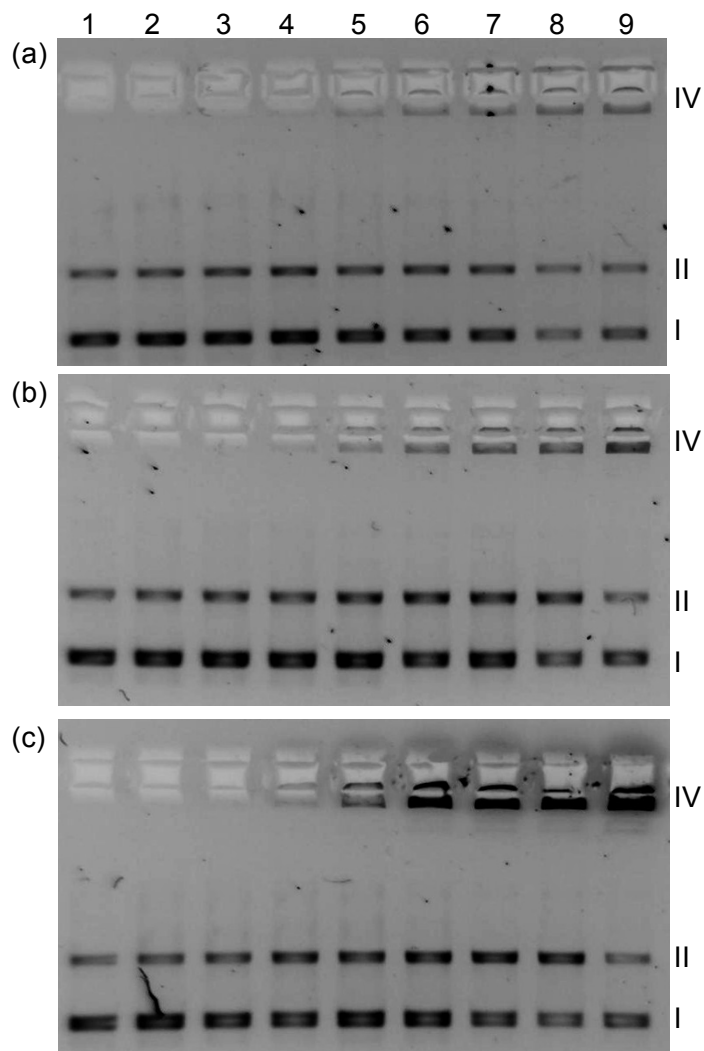


Fig. S12 DNA photocleavage of pUC19 DNA (20 μM bases) dosed with metal complex (MC) **1** (a), **2** (b) or **3** (c) and visible light (14 J cm^{-2}). Gel mobility shift assays employed 1% agarose gels ($0.75 \mu\text{g mL}^{-1}$ ethidium bromide) electrophoresed in $1\times$ TAE at 8 V cm^{-1} for 30 min. Lane 1, DNA only ($-h\nu$); lane 2, DNA only ($+h\nu$); lane 3, $5 \mu\text{M}$ MC ($+h\nu$); lane 4, $20 \mu\text{M}$ MC ($+h\nu$); lane 5, $40 \mu\text{M}$ MC ($+h\nu$); lane 6, $60 \mu\text{M}$ MC ($+h\nu$); lane 7, $80 \mu\text{M}$ MC ($+h\nu$); lane 8, $100 \mu\text{M}$ MC ($+h\nu$); lane 9, $100 \mu\text{M}$ MC ($-h\nu$). Forms I, II, and IV DNA refer to supercoiled plasmid, nicked circular plasmid, and aggregated plasmid, respectively.